Roles of IP_3 signaling in Wnt-regulated asymmetric divisions of *C. elegans* epithelial stem cells

Naoki YOSHIDA

Doctor of Philosophy

Multicellular Organization Laboratory, Structural Biology Center, National Institute of Genetics

Department of Genetics, School of Life Science

The Graduate University for Advanced Studies

2014 (School Year)

List of Contents

Abbreviations

APC	Adenomatous polyposis coli
APR-1	APC related protein
ajm	Apical junction molecule
AP	Anterior-posterior
C. elegans	Caenorhabditis elelgans
Ca^{2+}	Calcium ion $^{2+}$
cam-1	CAN cell migration defective
cdc-42	Cell division cycle 42
cDNA	complementary DNA
csnk-1	Casein kinase 1 gamma
cwn-1/-2	*C. elegans* Wnt1/2
DV	Dorsal-ventral
DG	Diacylglycerol
DNA	Deoxyribonucleic acid
ER	Endoplasmic reticulum
egl-20	Egg laying variant 20
Fz	Frizzled
GCaMP	GFP-Calmodulin-M13 Peptide
gf	Gain-of-Function
GFP	Green fluorescent protein
Hyp7	Hypodermal 7 syncytium
itr-1	Inositol 1,4,5-triphosphate receptor 1
IP_3	Inositol 1,4,5-triphosphate
IP_3R	Inositol 1,4,5-triphosphate receptor
L1/L2/L3/L4	Larval 1/2/3/4
lin-17/-18	abnormal cell lineage -17/-18
LSM	confocal laser scanning microscopy
mCherry	Monomeric Cherry
mg	Microgram
min	Minute
ml	Microliter

mm	Micrometer
mom-5	More of Ms
NGM	Nematode growth medium
PCP	Planer cell polarity
PCR	Polymerase chain reaction
PH domain	Pleckstrin homology domain
PI	Phosphatidylinositol
$PI(4,5)P_2/PIP_2$	Phosphatidylionositol-4,5-bisphosphate
plc-1/-2/-3/-4	Phospholipase C 1/2/3/4
PIP5K	Phosphatidylinositol-4-phosphate 5-kinase
PKC	Protein kinase C
POP-1	Posterior pharynx defect
ppk-1	Phosphatidylinositol phosphate kinase 1
RNA	Ribonucleic Acid
RNAi	RNA interference
rpm	Rotation per minute
Ror	Receptor-related
RT-PCR	Reverse transcription-polymerase chain reaction
Ryk	Receptor-like tyrosine kinase
sec	second
SSD	Salmon sperm DNA
TCF	T cell factor
unc	Uncoordinated
UV	Ultra Violet
Wnt	Wingless-Int
WntR	Wnt Receptor
WRM-1	Worm armadillo 1

Abstract

During development, asymmetric cell division is an important mechanism to generate cellular diversity and to maintain self-renewing stem cells. In *C. elegans* development, most somatic cells are polarized and divide asymmetrically to produce daughter cells with distinct fates. These asymmetric cell divisions are regulated by the Wnt/β-catenin asymmetry pathway that utilizes components similar to those of the canonical Wnt pathway. These components localize asymmetrically in the cell. For example, APR-1/APC localizes to the anterior cell cortex and regulates asymmetric nuclear localization of POP-1/TCF that localizes to the anterior daughter nucleus. Most somatic cells show the same POP-1 asymmetry and, hence, have the same polarity orientation. However, the mechanism to orient cell polarity is a mystery.

To reveal the mechanism that orients cell polarity, I focused on inositol 1,4,5-trisphoshate (IP_3) signaling that plays roles in regulating cell polarity. In this signaling, phosphatidylinositol-4-phosphate 5-kinase (PIP5K) produces phosphatidylinositol 4,5-bisphosphate (PIP_2), PIP_2 is hydrolyzed by phospholipase C (PLC) to produce IP_3. IP_3 binds to IP_3 receptor (IP_3R) causing to release of Ca^{2+} from endoplasmic reticulum (ER). This increased cytoplasmic Ca^{2+} in turn activate several cellular processes, resulting in regulation of cell polarity that is required for the direction of cell migration, the formation of cellular protrusions, and cell-cell adhesion. However, the relationship between asymmetric cell division and IP_3 signaling has not been studied directly.

I examined the *ppk-1*/PIP5K functions in seam cells which are epithelial stem

cells that repeatedly undergo self-renewing asymmetric cell divisions. Each seam cell is polarized and divides asymmetrically giving rise to an anterior daughter that is terminally differentiated to the hypodermal cell and a posterior one that remains in the seam cell fate. I found that *ppk-1(ok1411)* mutants had a defect in asymmetric cell divisions of seam cells by observing fates of daughter cells using *elt-3::*GFP (a hypodermal cell marker). Their daughter cell fates were swapped with each other compare to those in wild type (reversal phenotype). Furthermore, I found that the orientation of POP-1 asymmetry is also reversed in *ppk-1* mutants. These results indicate that that *ppk-1* regulates the polarity orientation of the seam cells. The reversal phenotype in *ppk-1* mutants was fully rescued by expression of PPK-1 under a seam cell specific promoter, suggesting that PPK-1 functions cell autonomously to regulate the cell polarity. I found that mCherry-tagged PPK-1 localizes symmetrically to the cell cortex and regulates the asymmetric localization of cortical APR-1/APC, judged by GFP-tagged APR-1. I revealed that IP_3 signaling components (PLC-4/PLC and ITR-1/IP3R) act downstream of PPK-1 by analyzing genetic interactions among these components. Based on these results, I conclude PPK-1 regulates the APR-1 polarity as a component of the IP_3 signaling pathway.

To further understand *ppk-1* function, I analyzed the genetic interactions between *ppk-1* and three Wnt genes. I found that the reversal phenotype in the *ppk-1* mutants is suppressed by loss-of-function mutations of *cwn-2*/Wnt. Furthermore, the reversal phenotype in *ppk-1* mutants was enhanced by the overexpression of CWN-2. These results suggest that the reversed polarity in *ppk-1* mutants is caused by *cwn-2*. In

contrast, in wild type, *cwn-2* promotes the normal orientation of cell polarity, suggesting that *cwn-2* has two functions promoting both the normal polarity orientation and the reversed polarity orientation. How does *cwn-2* have the two opposite functions? To answer this question, I analyzed the genetic interactions between *ppk-1* and six Wnt receptor genes. The reversal phenotype in *ppk-1* mutants was suppressed by each of *lin-18/*Ryk and *mom-5/*Frizzled mutations, suggesting that each of *lin-18* and *mom-5* is necessary to promote the reversal phenotype in *ppk-1* mutants. From these results, I conclude that *cwn-2* has two functions promoting both the reversed polarity orientation through the Wnt receptors (LIN-18 and MOM-5) and the normal polarity orientation depending on PPK-1 activities. Based on these results, I propose *ppk-1* is a switch that determines the CWN-2 function. Since IP_3 signaling and Wnt signaling are highly conserved among metazoans, similar mechanisms may also regulate proper cell polarity in other organisms.

Chapter

1

Introduction

1 Introduction

1-1 Asymmetric cell division

Asymmetric cell division (ACD) has an important role to generate cellular diversity during development and tissue regeneration. This division generates two daughter cells with distinct fates (Horvitz and Herskowitz, 1992). Because there are many examples of ACDs in developmental biology and stem cell biology, The ACD is not unique to animal development, to stem cells. In fact, bacterial and yeast cells divide asymmetrically, as do many cells in developing embryos (Amon, 1996; Goley et al., 2009; Laub et al., 2007). Therefore, the ACD is a ubiquitous feature of all organisms. However, many unanswered questions remain to be solved to understand mechanisms of ACDs.

1-2 Asymmetric cell division in *C. elegans*

C. elegans is one of the best-understood model systems for ACDs. During larval development, epithelial stem cells, called seam cells, undergo repeated self-renewing ACDs. Each of these ACDs produces a posterior daughter that remains as the seam cell and an anterior daughter that adapts terminally differentiate fate that fuses with the hyp7 syncytium (Sulston and Horvitz, 1977). One of the most important concepts in these ACD is that these cells have the same polarity orientation (Fig.1). However, mechanisms to orient the cell polarity are mystery.

1-3 The Wnt/β-catenin asymmetric (WBA) pathway

In *C. elegans*, most of ACDs are regulated by the Wnt/β-catenin asymmetry pathway (Mizumoto and Sawa, 2007; Siegfried et al., 2004; Walston et al., 2004). Each seam cell is polarized and divide asymmetrically, giving rise to an anterior daughter that terminally differentiates and a posterior one that remains in a seam cell fate. Our laboratory previously reported that the Wnt/β-catenin asymmetry pathway is essential for establishing ACDs of seam cells (Mizumoto and Sawa, 2007; Takeshita and Sawa, 2005; Yamamoto et al., 2011). This pathway utilizes components similar to those of the canonical Wnt pathway. In the WBA pathway, WRM-1/β-catenin and APR-1/APC localized to the anterior cell cortex to regulate the nuclear localization of WRM-1, resulting in its preferential localization to the posterior nucleus. This nuclear WRM-1 removes POP-1/TCF from the posterior nucleus, causing that POP-1 accumulates in the anterior nucleus. These asymmetric localizations are regulated by Wnt and Frizzled proteins (Fig. 2). Based on these asymmetries, all seam cells show the same POP-1 asymmetry and, hence, have the same polarity orientation. However, the mechanism to orient the cell polarity is a mystery.

1-4 IP_3 signaling pathway

Inositol 1,4,5-trisphoshate (IP_3) signaling is involved in regulation of cell polarity (Wei et al., 2009). In this signaling, phosphatidylinositol-4-phosphate 5-kinase (PIP5K) produces PIP_2, PIP_2 is hydrolyzed by phospholipase C (PLC) to produce IP_3. IP_3 binds to IP_3 receptors (IP_3Rs) causing release of Ca^{2+} from endoplasmic reticulum

(ER) (Fig. 3). This increased cytoplasmic Ca^{2+} in turn regulates many cellular processes, including cell polarization that are required for directed cell migration (Wei et al., 2009), the formation of cellular protrusions (Evans and Falke, 2007), cell-cell adhesion (Clapham, 2007; Pilipiuk et al., 2009), and convergent extension (Wallingford et al., 2001). In *C. elegans,* IP_3 signaling regulates a wide variety of physiological functions, including developmental morphogenesis (Pilipiuk et al., 2009; Thomas-Virnig et al., 2004), neuronal signaling (Walker et al., 2009), as well as rhythmic behaviors such as pharyngeal pumping (Walker et al., 2004), oocyte fertilization (Corrigan et al., 2005), defecation (Dal Santo et al., 1999), and male mating (Gower et al., 2005). However, relationships between IP_3 signaling and the ACD has not been reported.

1-5 New findings of this study

Here, I show that IP_3 signaling regulates the CWN-2/Wnt functions to correctly orient the seam cell polarity. First, Our laboratory performed RNAi screening to identify novel regulators of the WBA pathway. *ppk-1* was isolated as a result of its knockdown phenotype causing distal tip cell (DTC) hyperplasia which is also regulated by the WBA pathway. I found that a *ppk-1*/PIP5K mutation causes a reversed polarity orientation of seam cells, suggesting that *ppk-1* is a new regulator that orients the polarity. PPK-1 localizes symmetrically to the cell cortex and regulates the asymmetric localization of APR-1/APC at the cortex. I found that IP_3 signaling components (PLC-4/PLC and ITR-1/IP3 receptor) act downstream of PPK-1. Meanwhile, the *ppk-1* phenotype was suppressed by a mutation in *cwn-2*/Wnt, suggesting that *cwn-2* promotes

the reversed polarity in *ppk-1* mutants. In contrast, in wild type, *cwn-2* promotes the normal polarity, suggesting that *cwn-2* has two functions promoting both the normal and reversed polarity orientation. Based on my results, I conclude that *ppk-1* regulates the CWN-2 functions via IP_3 signaling to correctly orient the cell polarity.

Chapter

2

Materials and methods

2 Materials and Methods

2-1 Strains

Strains were derived from wild-type N2 Bristol strain and were cultured at 22.5°C on NGM plates and were fed with OP50 bacteria as described (Brenner, 1974). Double-mutant strains were constructed using standard genetic methods without additional marker mutations, except for *itr-1(sy290)* which marked with *unc-24(e138)* mutation. Mutations in the double mutants were confirmed by PCR and DNA sequencing.

In this study, the following alleles were mainly used: *ppk-1(ok1411), itr-1(sy290), plc-1(rx1), plc-2(ok1761), plc-3(tm1340), plc-4(ok1215), cwn-1(ok546) cwn-2(ok895), egl-20(n585), lin-17(n3091), cam-1(ks52), cfz-2(ok1201), mig-1(e1787), mom-5(ne12), lin-18(e620), cdc-42(gk388), unc-24(e138)* and *unc-76(e911)*.

Molecular information of tm allele are described in

http://www.shigen.nig.ac.jp/c.elegans/

Molecular information of all alleles except for tm allele is described in

http://www.cbs.umn.edu/CGC/index.html

2-2 Genotyping of *C. elegans* using PCR

To detect DNA mutations, worms were transferred into individual PCR tube with 20 μl worm lysis buffer containing Proteinase K (Wako) and incubate at 50 °C for one hour, which resulted in lysis of worms and release of genomic DNA. Proteinase K

was inactivated at 95 °C for 15 min. The worm lysate was used as templates for PCR with primers designed to distinguish between wild type and mutant alleles by producing two DNA fragments different in sizes or sequences.

2-3 Lineage analysis of seam cells

Lineage analyses were performed as described previously (Sulston and Horvitz, 1977). Seam cell nuclei were distinguished from hypodermal nuclei based on their morphology in addition to the expression of markers: *elt-3::GFP(vpIs1), scm::GFP(wIs51), or ajm-1::GFP+scm::GFP(wIs79)*. Since the V5.pa cell produces only neural cells that do not express these markers, I did not analyze polarity of the V5.pa division. Samples were prepared by immobilizing L2 stage hermaphrodites with 50 mM sodium aside and by placing them on 2% agarose pads. A Zeiss LSM700 microscope equipped with a 60x objective was used to examine cell fates of Vn.p cell daughters. Each strain was scored twice independently.

2-4 Confocal microscopy and data analysis

Confocal-microscopic images were obtained with Zeiss LSM700 equipped with a 488 nm and 561 nm lasers. Images of whole worms were complied using Adobe Photoshop CS5 and ImageJ (http://imagej.nih.gov/ij/). Intensities of GFP in nuclei were measured by imageJ (http://imagej.nih.gov/ij/).

2-5 Time-lapse microscopy

For live observations of GCaMP animals, a focal plane through the center of the seam cells was chosen. Samples were prepared by immobilizing L2 stage hermaphrodites with 2 mM levamisole in M9 buffer by placing them on 5% agarose pads. For imaging, Zeiss AxioImager Z1 equipped with a confocal scanner unit (CSU-W1, Yokogawa Electric Corporation) and an sCMOS camera (Neo, Andor Technology) was used. Image processing was performed with ImageJ (http://imagej.nih.gov/ij/).

2-6 Statistical Analysis

Statistical analysis was performed with the Fisher exact test.

2-7 cDNA library: RNA isolation from *C. elegans* and RT-PCR

For *C. elegans* total RNA isolation, wild-type (N2) worms were collected from non-starved plates by washing them with M9 buffer several times and were frozen at -80 °C. To extract RNAs, I used PureLink ^{TM} RNA Mini Kit (Life technologies). All buffers and regents were form this kit. An equal amount of glass beads (212-300 mm, SIGMA, G9143) was added to the frozen worm pellets, and the tubes were put in a Micro Smash (SM-100, Tomy Seiko) three times for 15 sec at 3000 rpm, while keeping them always on ice. RNA purification was carried out using the PureLink^{TM} RNA Mini Kit (Life technologies).

The second step, conversion of RNA to DNA, was carried out using the superscript III Reverse Transcriptase (Life technologies) according to the manufacture's protocol. After the reverse transcriptase reaction was completed, the generated cDNA from the original single stranded mRNA was used as template in a standard PCR.

2-8 Construction of Plasmids

2-8-1 Translational genes

A full-length *ppk-1* cDNA was cloned from a *C. elegans* cDNA library (see 2-7) by PCR amplification using PrimeSTAR Max (Takara). Primers were designed based on the predicted WormBase sequence of F55A12.3. Full-length translational mCherry reporters for PPK-1 and $PH_{PLC\delta}$ (from Addgene) were generated using Infusion technique (Invitrogen) and inserted into Fire vector modified pPD95.75 vector. mCherry was fused to the N-terminal of the proteins. Expression of mCherry::PPK-1 and mChery::$PH_{PLC\delta}$ were driven by a 9 kb fragment of seam cell specific promoter (Koh and Rothman, 2001). Transgenic worms were generated by injecting DNAs into *unc-76(e911)* worms with DNA (Mello et al., 1991). A *unc-76*-rescuing plasmid (Bloom and Horvitz, 1997) was used as a transformation marker, and co-injected with the PPK-1 and $PH_{PLC\delta}$ plasmids. The mCherry::PPK-1 and mChery::$PH_{PLC\delta}$ plasmids were injected at 10 ng/ml together with 50 ng/ml of the *unc-76* plasmid and 40 ng/ml of salmon sperm DNA (SSD) (life technologies). Transgenic animals produced by injection typically carry large extrachromosomal arrays that contain many copies of the co-injected DNAs.

Extrachromosomal arrays can be integrated into a chromosome. Integrated lines of worms expressing mCherry::PPK-1 and mCHerry::$PH_{PLC\delta}$ were generated by exposing 50 transgenic animals to a dose of 30,000 μJ/cm^2 of UV lights in CL-1000 Ultraviolet Crosslinker (Uutra-Violet products). Irradiated animals were grown until

their stervation on 9 cm plates five times. After this, one hundred nonUnc offspring were isolated. Each of integrated lines, *osIs91* (*Pscm*::mCHerry::PPK-1; *unc-76*) and *osIs90* (*Pscm*::mCherry::PHPLCδ; *unc-76*) were then identified by segregation of 100% nonUnc and mCherry-positive animals.

2-8-2 A transcriptional fusion gene

*plc-4::*Venus construct. 1.855 kb of upstream *plc-4* promoter and 2.981 kb of *plc-4* gene were amplified from wild-type genomic DNA using the following primers:
plc-4-F: 5'-GTGCCCAAAGCACTCTAATCGG-3'. And
plc-4-R: 5'-GTACTCTTCCTCCATTGCAATTCGTAC-3'.

By using Infusion technique (life technologies), the PCR fragment was cloned into modified-pPD95.75 vector in which GFP was replaced by Venus. The *plc-4::*Venus plasmid was injected at 10 ng/ml together with 50 ng/ml of unc-76 and 40 ng/ml of SSD. The resulting array is osEx523.

Chapter

3

Results

3 RESULTS

3-1 *ppk-1*/PIP5K is required for asymmetric cell division

Lateral seam cells are specialized epithelial stem cells. During each larval stage, each of these seam cells is polarized and divides asymmetrically to give rise to an anterior daughter that fuses with hyp7 epidermal syncytium and a posterior daughter that remains as a seam cell (Fig. 1).

To understand roles of IP_3 signaling in asymmetric division of seam cells, I examined *ppk-1*/PIP5K mutants. To analyze fates of the seam cell daughters, I used *elt-3::GFP(vpIs1)*, which is expressed in the hyp7 epidermal syncytium but not in seam cells (Gilleard et al., 1999; Koh and Rothman, 2001) (Fig. 4A). I then analyzed the lineage of seam cells during each larval stage. Although *ppk-1(ok1411)* mutants showed normal daughter fates of seam cells during the L1 stage (Fig. 4C), At the L2 and L3 stages, I found that *ppk-1(ok1411)* mutants had a defect in ACDs of some seam cells (Fig. 4 DE). This defect is that the fates of the daughter cells were swapped with each other compare to those in wild type (Fig. 4B). Hereafter I call this phenotype as 'reversal phenotype'. The reversal phenotype was observed in specific seam cells at each stage. At the L2 stage, reversal phenotype was observed in V2.pa cell, but not in V2.pp cell, even though these cells are V2.p cell daughters and have same cell lineages (Fig. 4D). At the L3 stage, the reversal phenotype was observed in seam cells that are located in anterior side of animal body (Fig. 4E). I could not analyze the phenotype at the L4 stage, because *ppk-1(ok1411)* mutants arrest their development at the late L3 stage. In contrast to the reversal phenotype, *ppk-1(ok1411)* mutants did not show

symmetric cell divisions, suggesting that *ppk-1* is important to orient the cell polarity but not to generate it. Because the V2.pa cell division showed the strongest reversal phenotype, hereafter I focused on the ACD of the V2.pa cell (Fig. 4 DE).

I next conducted a cell-specific rescue experiment to examine the cell autonomy of the *ppk-1* function. The reversal phenotype was fully rescued by the expression of PPK-1 under the seam cell-specific promoter (*scm* promoter) (Fig. 5A). No rescue was observed when PPK-1 was expressed with the pharynx-specific promoter (*myo-2* promoter) (Fig. 5A). It was reported previously that GFP was expressed under the control of *ppk-1* promoter, *Pppk-1*::GFP*(gqEx33)*, is expressed in seam cells in adult hermaphrodites (Weinkove et al., 2008). I found that *Pppk-1*::GFP*(gqEx33)* is also expressed in seam cells at the L2 stage (Fig. 5B). These results indicate that *ppk-1* functions cell autonomously in the seam cells to regulate ACDs.

3-2 *ppk-1* regulates localizations of the WBA pathway components

In *C. elegans*, ACDs of seam cells are regulated by the WBA pathway. Components of this pathway include WRM-1/β-catenin, APR-1/APC and a POP-1/TCF transcription factor (Mizumoto and Sawa, 2007) (Fig. 2A). During cell divisions, WRM-1 and APR-1 are localized asymmetrically to the anterior cortex in the mother cell (Mizumoto and Sawa, 2007; Nakamura et al., 2005). After a cell division, nuclei of the anterior and posterior daughters have more POP-1 and WRM-1 than the other nuclei, respectively (Fig. 2B).

As shown above, *ppk-1* is important in asymmetric divisions of some seam

cells. However, *ppk-1* has not been implicated in the WBA pathway previously. To examine whether *ppk-1* regulates the localizations of the WBA pathway components, I first analyzed the POP-1/TCF localization. I used a transgene GFP::POP-1(*qIs74*) (Siegfried et al., 2004). POP-1 normally accumulates in the anterior daughter nucleus in wild type. In *ppk-1* mutants, I found that GFP::POP-1 asymmetry was reversed about 42% in V2.pa daughters in *ppk-1(ok1411)* mutants (Fig. 6AB). These results indicate that *ppk-1* controls the cell polarity via the WBA pathway.

Because the asymmetric localization of GFP::POP-1 requires nuclear WRM-1/β-catenin (Lo et al., 2004), I observed the asymmetric localization of WRM-1 in daughter nuclei by using WRM-1::GFP (*osIs5*) (Mizumoto and Sawa, 2007). WRM-1 normally accumulates in the posterior daughter nucleus in wild-type animals (Nakamura et al., 2005; Takeshita and Sawa, 2005) (Fig. 7A). This asymmetry was reversed about 20% in *ppk-1(ok1411)* mutants (Fig. 7AB), suggesting that *ppk-1* functions upstream of nuclear WRM-1.

Because the asymmetric localization of WRM in daughter nuclei requires the anterior cortical localization of WRM-1 and APR-1 in their mother cell (Mizumoto and Sawa, 2007). I observed the localization of cortical APR-1 by using APR-1::GFP*(osIs13)* (Mizumoto and Sawa, 2007). While APR-1::GFP normally accumulated on the anterior-daughter cortex of seam cells in wild-type animals (Fig. 8A), APR-1::GFP was not asymmetrically localized in V2.pa cell in *ppk-1(ok1411)* mutants (Fig. 8B). Next I observed the localization of WRM-1 by using WRM-1::GFP(*osIs5*). I could not distinguish the discrepancy of the cortical WRM-1

localization between wild type and *ppk-1(ok1411)* mutants, because WRM-1::GFP localization was randomized in Vn.pa cells including V2.pa cell in wild type (Fig. 8C). I conclude that *ppk-1* regulate at least cortical polarity of APR-1 in V2.pa cell.

3-3 *ppk-1* localizes to the cell cortex

To further characterize the role of *ppk-1* in Wnt-regulated ACDs, I analyzed PPK-1 subcellular localization in seam cells. I expressed a mCherry-tagged PPK-1 in seam cells by using the *scm* promoter. mCherry-tagged PPK-1 is functional, because its expression can rescue the reversal phenotype of *ppk-1* mutants (Fig. 5A). In all cell-cycle including the interphase, prophase, metaphase and telophase, PPK-1::mCherry is localized uniformly to the cell cortex (Fig. 9ABC). Thus, the subcellular localization of PPK-1 is consistent with its role in regulation of cortical polarity.

3-4 *ppk-1* functions in the IP_3 signaling pathway

To understand the molecular mechanism underlying the regulation of the cortical APR-1 asymmetry mediated by *ppk-1*, I analyzed genetic interactions between *ppk-1* and IP_3 signaling components. Since a gain of function (*gf*) mutation of *itr-1*/IP3R is able to suppress the sterility of *ppk-1(RNAi)*, *itr-1* is downstream effector of *ppk-1* (Fig. 3) (Xu et al., 2007). This *itr-1(sy290gf)* allele carries a missense mutation in IP_3 binding domain of ITR-1/IP3R (Clandinin et al., 1998).

To examine whether the asymmetric division of the seam cell is linked to the

IP_3 signaling pathway, I observed the *ppk-1(ok1411)* phenotype in the *itr-1(sy290gf)* background. *ppk-1(ok1411); itr-1(sy290gf)* mutants displayed weaker reversal phenotype (15%) than *ppk-1* single mutants (46%) (Fig. 10), suggesting that the reversal phenotype in *ppk-1(ok1411)* mutants is suppressed by the *itr-1(sy290gf)* mutation and that *ppk-1* functions through IP_3 signaling.

Phospholipase C (PLC) is necessary for producing IP_3 from PIP_2. I hypothesized that the disruption of the PLC function should result in the reversal phenotype of the seam cell as in *ppk-1* due to the decrease of IP_3 signaling. I tested functions of four genes encoding PLCs (*plc-1, plc-2, plc-3, and plc-4*) (Fig. 11). Among the four PLCs, a mutation of only the *plc-4* gene showed the reversal phenotype in the seam cell. Thus, *plc-4* activity is required for the proper ACD in the seam cell. Depletion of *plc-1, plc-2, and plc-3* had no effects on the ACD in seam cells. To elucidate the relationship between *ppk-1 and plc-4*, I analyzed cell fates of *ppk-1; plc-4* double mutants. *ppk-1; plc-4* double mutants did not suppress, nor enhanced the reversal phenotype compare to those in *ppk-1* mutants, suggesting that both *ppk-1* and *plc-4* function in the IP_3 signaling pathway (Fig. 11). Based on these results, it is suggested that *ppk-1* functions in the ACD in through IP_3 signaling.

3-5 *plc-4* is highly expressed in seam cells

To examine the expression pattern of *plc-4,* I generated transgenic worms expressing full-length PLC-4 fused to Venus. This expression was driven by a 1.9-kb fragment of the *plc-4* promoter located immediately upstream of the start codon (Fig 12A).

Prominent expression of PLC-4::Venus was detected in hypodermal seam cells, intestine, body wall muscles, and excretory cells in L2 larvae (Fig. 12B). Weaker expression was seen in the pharynx and some neurons. Similar expression pattern was partially described in previous study (Vazquez-Manrique et al., 2010). PLC-4::Venus localized to the cortex of seam cells (Fig. 12C). Thus, the subcellular localization of PLC-4 is consistent with its role in the regulation of polarity orientation of the seam cell.

3-6 Ca^{2+} imaging in seam cells

Based on the genetic interaction between *ppk-1* and the calcium channel ITR-1, I expected involvements of Ca^{2+} in the ACD. To analyze Ca^{2+} dynamics in seam cells, I used a Ca^{2+} sensor GCaMP3 which has been used in *C. elegans* neurons and hypodermal cells to image calcium transients (Tian et al., 2009; Xu and Chisholm, 2011).

I established transgenic worms expressing GCaMP3 under the control of the *scm* promoter. Although I succeeded to observe Ca^{2+} dynamics only in three animals, in all cases, I found that GCaMP3 fluorescence repeatedly spreads from V1.pa cell to V6.pp cell like waves (n=3) (Fig. 13). This result raises a possibility that Ca^{2+} dynamics orients the polarity of seam cells.

3-7 *cdc-42* may be a downstream effector of *itr-1*

In the *Xenopus* embryo, Cdc42 functions downstream of IP_3 signaling which

activates IP_3R to express Ca^{2+} to cytoplasm. An increase of intracellular Ca^{2+} activates PKC (Sheldahl et al., 2003) that regulates small GTPase Cdc42 (Schlessinger et al., 2007). In addition, Cdc42 is a major regulator of cell polarity from yeast to mammalian cells (Etienne-Manneville, 2004). From these data, I hypothesized that *cdc-42* regulates cell polarity as a down stream effector of IP_3 signaling.

I found that *cdc-42(gk388)* animals showed the reversal phenotype similar to *ppk-1(ok1411)* animals (Fig. 14AB). To examine whether *cdc-42* is a downstream effector of *itr-1*, I analyzed *cdc-42(gk388)*; *itr-1(sy290gf)* double mutants. *itr-1(sy290gf)* fails to suppress the reversal phoenotype defect of *cdc-42(gk388)* (Fig. 14C). This result may suggest that *cdc-42* is a downstream effector of *itr-1* to orient the polarity orientation of the seam cell.

3-8 *ppk-1* genetically interacts with *cwn-2/Wnt*

The polarity orientation of seam cells at L1 stages is redundantly regulated by Wnts (*cwn-1, cwn-1,* and *egl-20*) (Yamamoto et al., 2011). My results suggest that *ppk-1* also regulates the polarity orientation of the V2.pa cell. I next examined genetic interactions between *ppk-1* and three Wnt genes (*cwn-1, cwn-2,* and *egl-20*). I found that the reversal phenotype of *ppk-1(ok1411)* mutants was suppressed by *cwn-2(ok895)* or *cwn-2(RNAi)*, but not by mutations in the other Wnt genes (*cwn-1(ok546)* and *egl-20(n585))* (Fig. 15). These epistatic relationships suggest that *ppk-1* functions upstream of or in parallel to *cwn-2*. It is unlikely, however, that *ppk-1* functions upstream of *cwn-2*. As described above, *ppk-1* functions cell-autonomously, whereas

Wnt proteins including CWN-2 are believed to act in a non-cell autonomous manner (Clevers, 2006). In addition, CWN-2 expressed specifically in the pharynx can regulate the polarity of seam cells (Yamamoto et al., 2011). Therefore, these observations suggest that *ppk-1* functions in parallel to *cwn-2* signaling rather than downstream of it.

The reversal phenotype in *ppk-1(ok1411)* mutants was enhanced by the overexpression of CWN-2 (Fig. 15). These results suggest that the reversed polarity in *ppk-1* mutants depends on CWN-2. Therefore, CWN-2 functions to promote reversed orientation of the polarity in *ppk-1* mutants. In contrast, in the presence of normal *ppk-1* function, *cwn-2* promotes the normal orientation of the polarity at least in the L1 stage (Yamamoto et al., 2011). These results suggest that *cwn-2* has two functions promoting normal and reversed polarity orientation, depending on the PPK-1 activities.

3-9 *ppk-1* genetically interacts with *lin-18*/Ryk and *mom-5*/Frizzled

How does *cwn-2* have the opposite functions? I hypothesized that these *cwn-2* functions are mediated by different Wnt receptors. To examine this hypothesis, I analyzed genetic interactions between *ppk-1(ok1411)* and six Wnt receptor genes (*mom-5(ne12), cfz-2(ok1201), lin-17(n3091), mig-1(e1787), cam-1(ks52),* and *lin-18(e620)*). I found that the reversal phenotype in *ppk-1* mutants was suppressed in the *lin-18* or *mom-5* backgrounds. Mutations of other Wnt receptor genes did not modify the reversal phenotype of *ppk-1* (Fig. 16). These results suggest that *lin-18* and *mom-5* are necessary to promote the reversal phenotype in *ppk-1* mutants.

3-10 Overexpression of CWN-2 promotes the reversed polarity in *ppk-1* mutants

In L2 stage, only V2.pa cell showed reversal phenotype in *ppk-1* mutants (Fig. 17D). As shown above, this reversal phenotype is suppressed by *cwn-2* mutation in *ppk-1* mutants. To examine whether overexpression of CWN-2 causes the reversal phenotype in other seam cells. I expressed CWN-2 in the anterior side of the animals by using *Pcwn-2::*CWN-2::Venus(*osIs23*) in *ppk-1* mutants. I found that overexpression of CWN-2 in *ppk-1* mutants caused the reversal phenotype in the anterior seam cells (V1.pa and V3.pa cells) that are not affected in *ppk-1* single mutants. Next, I expressed CWN-2 in the posterior side of animals by using *Pegl-20::*CWN-2::Venus*(osEx398)* in *ppk-1* mutants to find that V6.pa and V4.pa cells located in the posterior side of the animals showed the reversal phenotype (Fig. 17AC). These results suggest that the CWN-2 has a potential at least weakly to reverse the polarity of some seam cells in *ppk-1* mutants. *Pegl-20::*CWN-2::Venus rescued the polarity defect of all seam cells in triple Wnt mutants at the L2 stage (Fig. 18AB), as reported for L1 seam cells (Yamamoto et al., 2011). However, *Pegl-20::*CWN-2*::*Venus*(osEx398)* did not strongly promotes the reversal phenotype of seam cells in *ppk-1* mutants (Fig. 17C). These results suggest that CWN-2 is not sufficient to reverse the polarity orientation in *ppk-1* mutants.

3-11 Overexpression of LIN-18 promotes the reversed polarity in *ppk-1* mutants

CWN-2 is not sufficient to reverse the polarity orientation in *ppk-1* mutant, suggesting that other components are also required for the reversal phenotype in *ppk-1*

mutants. As shown above, I found that *lin-18* and *mom-5* are required for the reversal phenotype of the V2.pa cell in *ppk-1* mutants (Fig. 16). At the L2 stage, *mom-5::*Venus*(osEx524)* is expressed in all seam cells (Fig. 19A). In contrast, *lin-18::GFP(syIs75)* is expressed in V1.pn, V2.pn and V3.pn cells that are located in the anterior-side of the animals at the L2 stage (Fig. 19B). In other words, *lin-18* is not expressed in the posterior side of the animals. I hypothesized that animals that express LIN-18 in all seam cells should cause the reversal phenotype in all seam cells of *ppk-1* mutants. To examine this hypothesis, I expressed LIN-18 in all seam cells by expressing it under the *scm* promoter in *ppk-1* mutants. These animals showed the reversal phenotype (in addition to rare symmetric divisions) in V1.pa, V3.pa and V5.pa cells that did not show the phenotype in *ppk-1* single mutants (Fig. 19C). This result suggests that expression of LIN-18 is important for the reversal phenotype in *ppk-1* mutants. Because CWN-2 is expressed only in the anterior side of the animals, Next I expressed *Pegl-20::*CWN-2*::*Venus and *Pscm::*LIN-18::Venus in *ppk-1* mutants. These animals showed that the reversal phenotype and symmetric cell division, but these phenotypes are at low frequencies (Fig. 19D). These results suggest that CWN-2 and LIN-18 are not sufficient for the reversal phenotype in *ppk-1* mutants, and that some downstream components might be required for CWN-2 to cause this phenotype.

Chapter 4

Discussion

4 Discussion

4-1 Summary of results

My results establish *ppk-1* as a new regulator of the ACD regulated by the WBA pathway. *ppk-1(ok1411)* mutants showed the reversal phenotype, suggesting that *ppk-1* regulates the polarity orientation of the ACD. The experiments of molecular imaging revealed that *ppk-1* localizes to the plasma membrane and regulates the cortical polarity of APR-1. From genetic interaction analyses, I found that IP_3 signaling components (*plc-4*/PLC and *itr-1*/IP3R) act downstream of *ppk-1*, suggesting that *ppk-1* regulates the APR-1 polarity by regulating the function of the IP_3 signaling pathway. Further genetic interaction analyses revealed that *ppk-1* interacts genetically with *cwn-2*/CWN-2, *lin-18*/Ryk and *mom-5*/Frizzled, suggesting that these components promote the reversed polarity. All my results suggest that *ppk-1* has a novel function to regulate the polarity orientation in seam cells.

4-2 *ppk-1* is linked to IP_3 signaling to regulate the ACD

ppk-1(ok1411) induced the reversal phenotype was suppressed by the *itr-1(sy290gf)* background (fig. 10). The *sy290* mutation is a gain-of-function causing ITR-1/IP_3R to be constitutively active or more sensitive to IP_3 than wild type (Clandinin et al., 1998). This result suggests that ITR-1 activity is important for regulating the polarity orientation in the *ppk-1* function to regulate the cell polarity orientation. Activated ITR-1 releases Ca^{2+} from the smooth ER, causing an elevated cytoplasmic Ca^{2+} concentration. Therefore the increased Ca^{2+} most likely contribute to orient the

proper polarity of the seam cell in PPK-1 function.

4-3 A model for PPK-1 function

My results revealed, depending on the *ppk-1* activities, CWN-2 has two functions promoting normal and reversed polarity of the seam cell. I call these functions as 'normal CWN-2 function' and 'reversed CWN-2 function' (Fig. 20A). The reversed CWN-2 function was observed in *ppk-1(ok1411)* mutants, but not in wild type. These results suggest that the CWN-2 functions are regulated by PPK-1 to correctly orient the polarity. How does *cwn-2* have the two opposite functions? My results suggest that each of *lin-18* and *mom-5* is necessary to promote the reversal phenotype in *ppk-1* mutants. In contrast, in wild type, *lin-17, cam-1,* and *mom-5* are redundantly required for the normal polarity at least L1 stage (Yamamoto et al., 2011). How does PPK-1 control the polarity orientation? My results suggest that *ppk-1* functions via IP_3 signaling to regulate seam cell polarity. IP_3 signaling regulates Ca^{2+} expression from ER. Then Ca^{2+} expression may be decreased in *ppk-1* mutants. Based on these data, I propose a model to explain the *ppk-1* function. In this model, there are two pathways. One pathway is that increased Ca^{2+} concentration activates the normal CWN-2 function through the Wnt receptors (LIN-17, CAM-1, and MOM-5) (Fig. 20A: Pathway 1). In this case, the activity of the normal CWN-2 function is higher than the reversed CWN-2 function. Then the cell shows the normal polarity in its ACD. In *ppk-1* mutants, the activity of the normal CWN-2 function is downregulated. Then these animals showed the reversal phenotype. The second pathway is that increased Ca^{2+} concentration inhibits the

reversed CWN-2 function through Wnt receptors (LIN-18 and MOM-5) (Fig. 20A: Pathway 2). In this model, only the normal CWN-2 function is activated by CWN-2. In *ppk-1* mutants, both CWN-2 functions are activated. Then these animals showed the reversal phenotype.

4-4 Downstream components of IP_3 signaling to regulate the ACD

This study demonstrated that *ppk-1* is linked to *itr-1* and the WBA pathway, suggesting that *ppk-1* mediates IP_3 signaling to regulate the ACD. ITR-1 is required for Ca^{2+} expression from ER in response to IP_3. It is unclear that how ITR-1 modulates the polarity orientation of the cell. In *Xenopus* embryo, small GTPase Cdc42 functions downstream of IP_3 signaling. An increase of intracellular Ca^{2+} activates cPKC (Sheldahl et al., 2003). Then, ITR-1 positively regulates Cdc42 (Schlessinger et al., 2007). Cdc42 is the key effector of the planer cell polarity (PCP) pathway to remodel actin cytoskeleton (Schlessinger et al., 2007). My results showed that *cdc-42* caused small percentage of the reversal phenotype in seam cells and that *itr-1(sy290gf)* fails to suppress the reversal phenotype of *cdc-42*, implicating that *cdc-42* is a downstream effector of *itr-1* to regulate polarity of seam cells.

4-5 Why do *ppk-1* mutants show the reversal phenotype only in specific cells?

The reversal phenotype of *ppk-1* mutants was observed in specific cells at the L2 and L3 stages, but not at the L1 stage. At the L3 stage, seam cells that located anterior side of animals showed this phenotype (V1.pap, V1.ppp, V2.pap, and V3.pap)

(Fig. 4E). At the L2 stage, only V2.pa cell showed this phenotype (Fig. 4D). All the cells that showed the reversal phenotype expressed LIN-18. Furthermore, all the cells that showed the normal polarity did not express LIN-18, suggesting that *lin-18* is necessary to promote the reversed polarity. LIN-18 was previously reported to re-orient P7.p and to reverse the AP pattern of nuclear TCF/POP-1 levels in P7.p daughters (Deshpande et al., 2005; Inoue et al., 2004), suggesting that LIN-18 have a potential to reverse the polarity. This is consistent with my finding that LIN-18 is necessary to promote the reversal phenotype in *ppk-1* mutants. Whether is LIN-18 sufficient to reverse the polarity orientation? Ectopic expression of LIN-18 in seam cells promotes the reversed polarity in some Vn.pa cells in *ppk-1* mutants, but not in all seam cells (Fig. 19C). This result suggests that LIN-18 is not sufficient for the reversal phenotype in *ppk-1* mutants. To clearly explain why *ppk-1* mutants show the reversal phenotype only in specific cells, further analysis is necessary to identify the components to promote the cell polarity.

4-6 IP_3 signaling and cell polarity in other organisms

IP_3 signaling regulates the Ca^{2+} release from ER. This increased cytoplasmic Ca^{2+} in turn activate several cellular processes, resulting to regulate cell polarity. This polarity regulates the direction of cell migration (Wei et al., 2009), the formation of cellular protrusions (Evans and Falke, 2007), cell-cell adhesion (Clapham, 2007), and convert extension (Wallingford et al., 2001). Then IP_3 signaling may be a ubiquitous regulator of the cell polarity, Since IP_3 signaling and Wnt signaling are highly

conserved among metazoans, similar mechanisms may also regulate proper cell polarity in other organisms.

4-7 The significance of this study

The ACD is a ubiquitous feature of all organisms. In *C. elegans*, the WBA pathway orients the cell polarity of seam cells to promote proper ACDs. This work provides new insight into the mechanism that orients the cell polarity. I showed that IP_3 signaling components is required for the proper localization of cortical APR-1. As shown above, IP_3 signaling is involved in regulation of the cell polarity in many developmental events. IP_3 signaling may be important regulator of cell polarity orientation in animal development.

Chapter 5

Figures

5 Figures

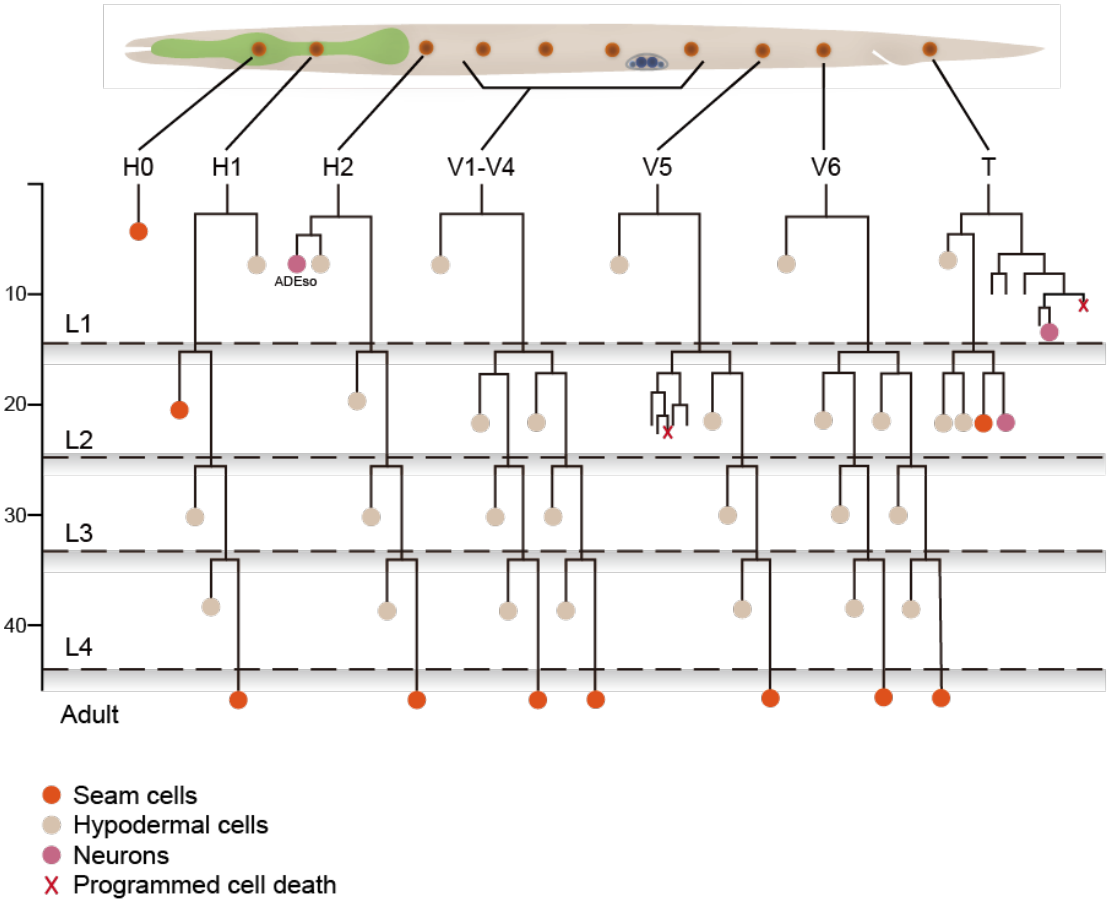

Figure 1. Epithelial stem cells in *C. elegans*

Division patterns of epithelial stem cells during larval stages. Hours post hatching and larval stages are indicated on the left.

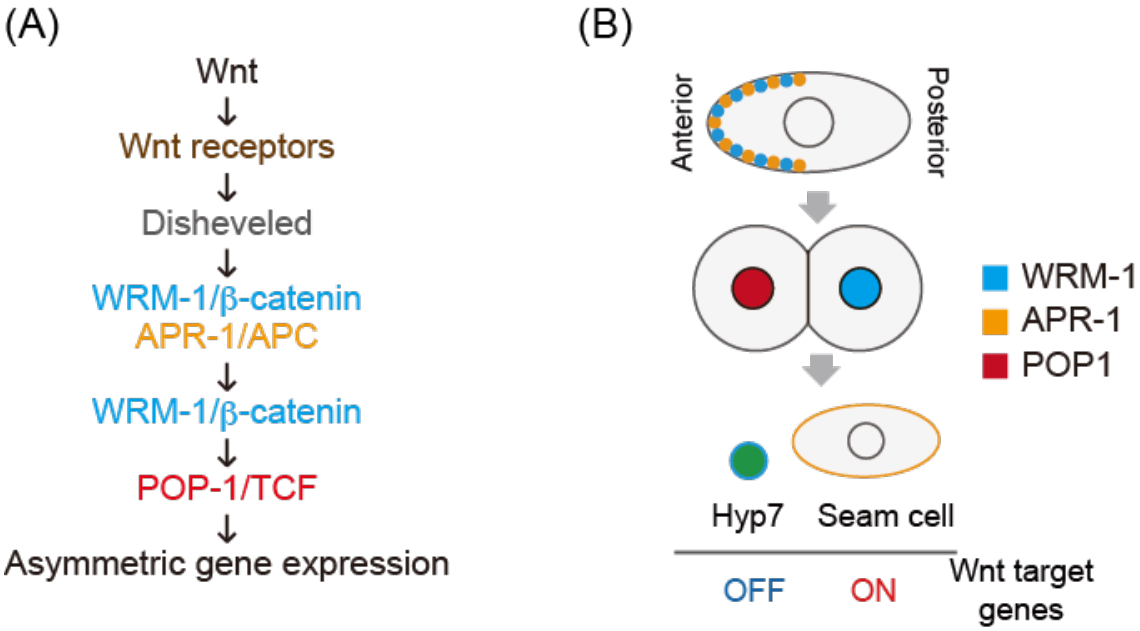

Figure 2. Introduction of the Wnt/β-catenin asymmetry (WBA) pathway

(A) A scheme of the WBA pathway.

(B) A schematic drawing of the localization of the WBA components during the seam cell division.

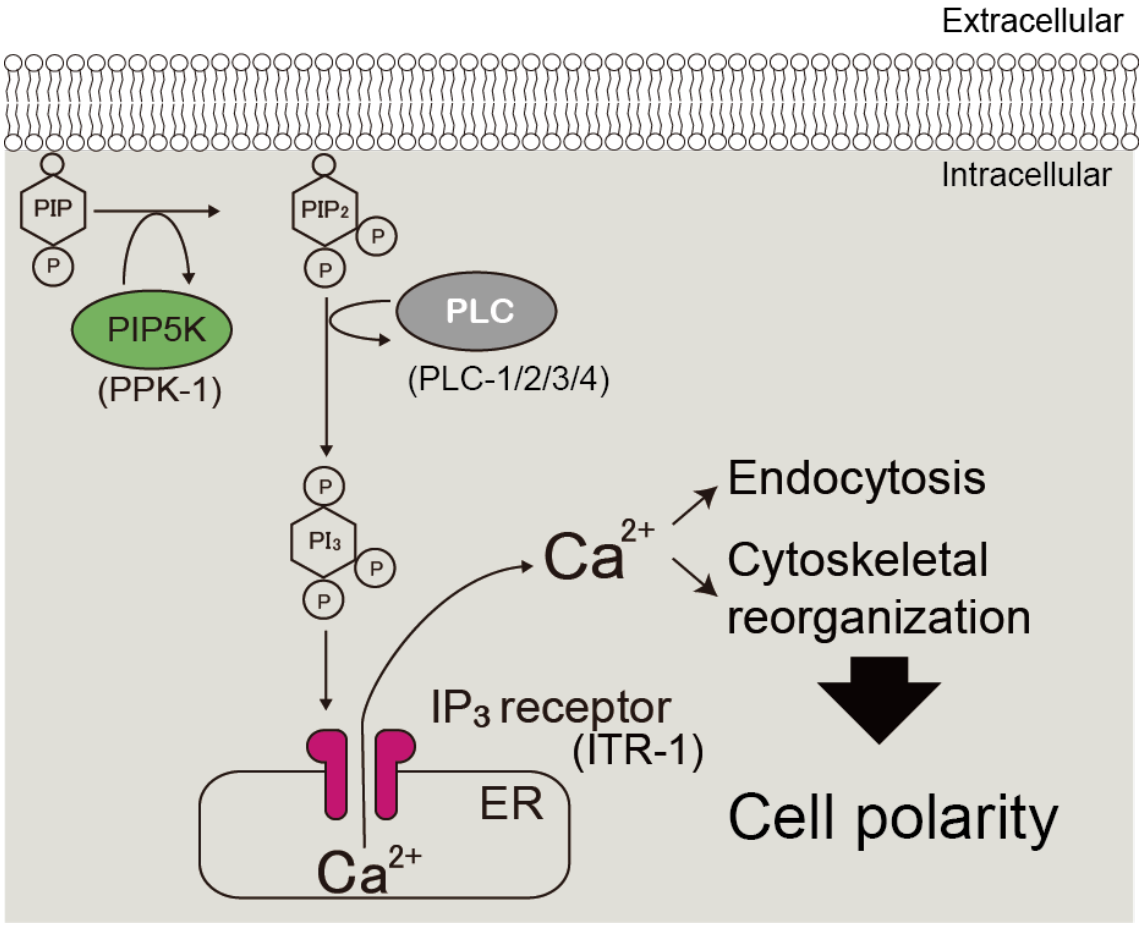

Figure 3. IP_3 signaling

A scheme of IP_3 signaling. Components of *C. elegans* homologs are noted in brackets.

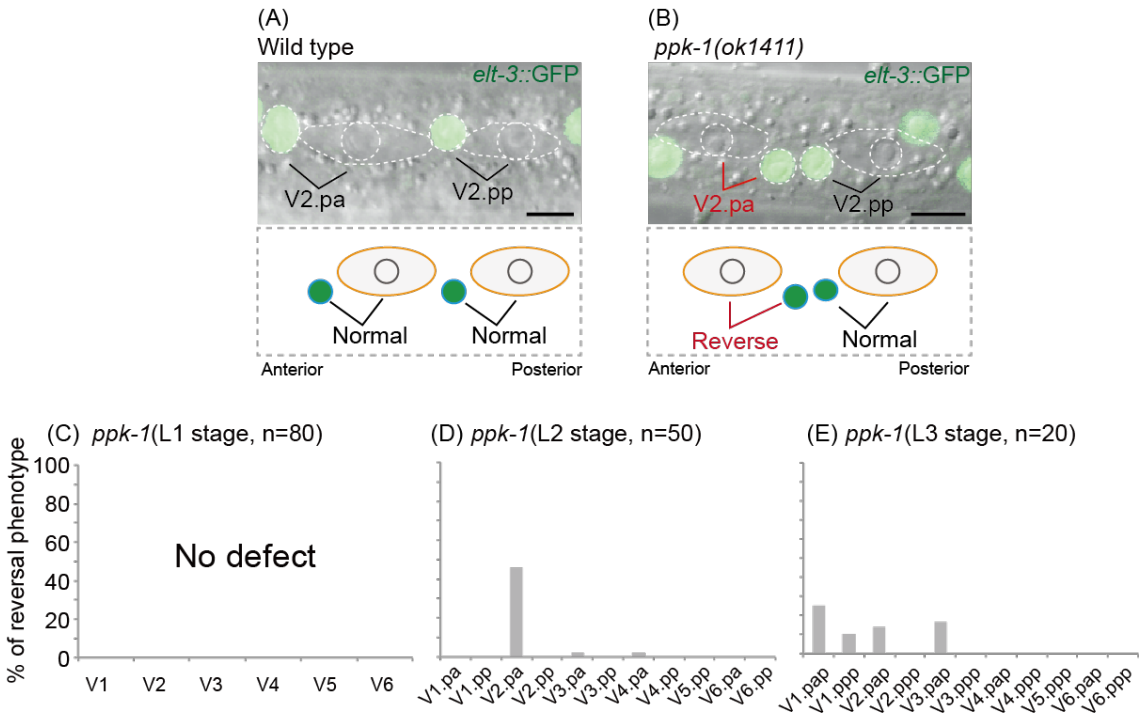

Figure 4. Analyses of the seam cell polarity in *ppk-1* mutants

(A, B) seam cells of the late L2 stage hermaphrodite visualized by *elt-3*::GFP.

(A) Wild type. The two seam cells divide asymmetrically. Daughter cells have the same polarity orientation.

(B) *ppk-1(ok1411)*. The division of the V2.pa cell is reversed (the fates of their daughter cells are exchanged with each other). Scale bars are 5 μm.

(C, D, E) Frequencies of the reversal phenotype in *ppk-1* mutants. (A) L1 stage. (B) L2 stage. (C) L3 stage.

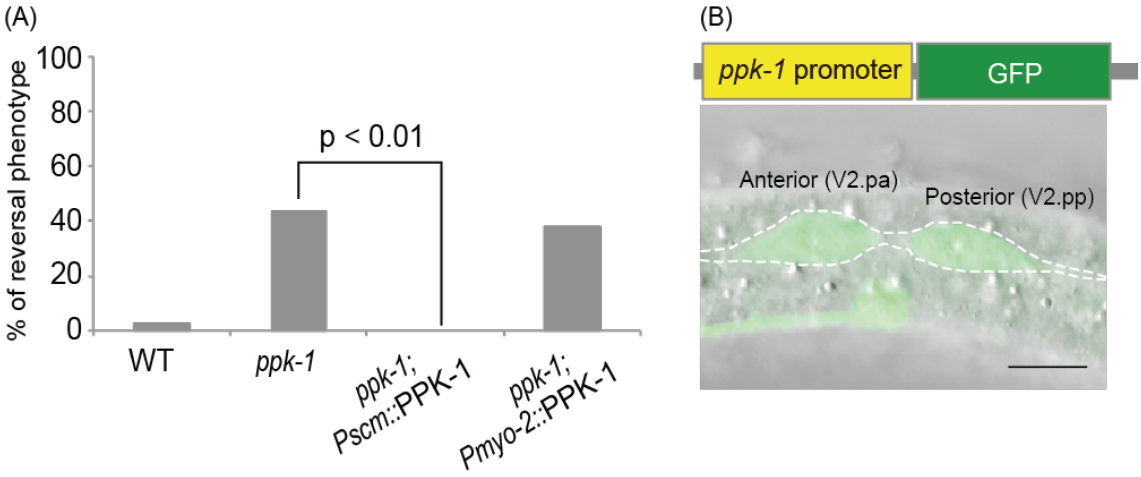

Figure 5. PPK-1 functions cell-autonomously and expressed in seam cells

(A) Frequencies of the reversal phenotype of V2.pa cell in wild type (n=81), *ppk-1(ok1411)* (n=53), *ppk-1*; *Pscm::mCherry::*PPK-1 (n=20), and *ppk-1*; *Pmyo-2::mCherry::*PPK-1 (n=21).

(B) *Pppk-1::*GFP was expressed in seam cells. Scale bar is 5 μm.

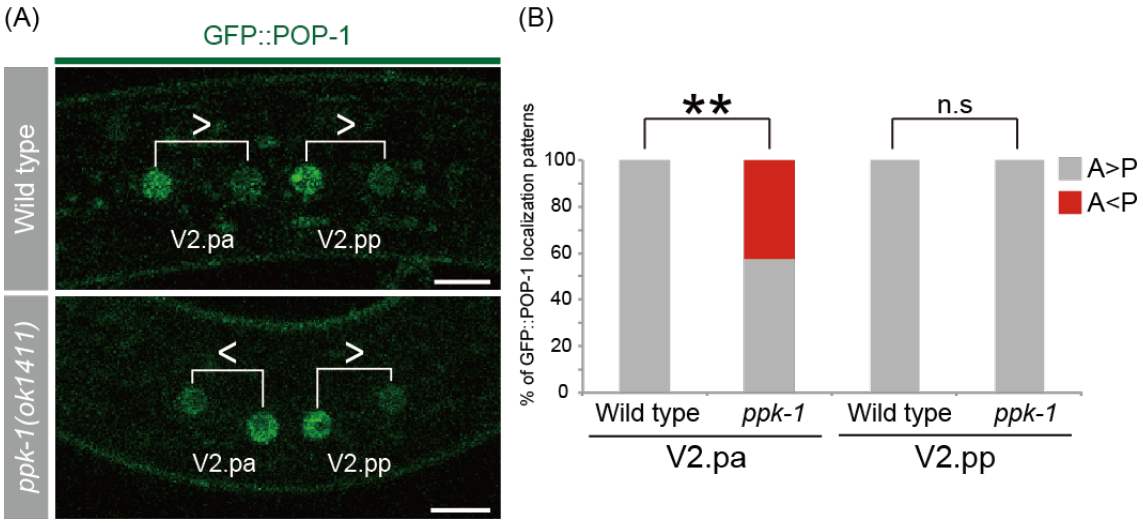

Figure 6. POP-1 localization patterns in daughter nuclei in wild type and *ppk-1(ok1411)* mutants

(A) Confocal images showing the localization of GFP::POP-1 in wild type (top), and *ppk-1(ok1411)* (bottom). Pairs of daughter nuclei are shown with brackets in each panel. The inequality signs indicate relative intensities of GFP::POP-1 levels between two daughters. Scale bars are 5 μm.

(B) Frequencies of the localization patterns of GFP::POP-1in wild type (n=20) and *ppk-1* (n=26). A, intensity of GFP::POP-1 at the anterior nucleus; P, intensity of GFP::POP-1 at the posterior nucleus. **, P<0.01. n.s., not significant.

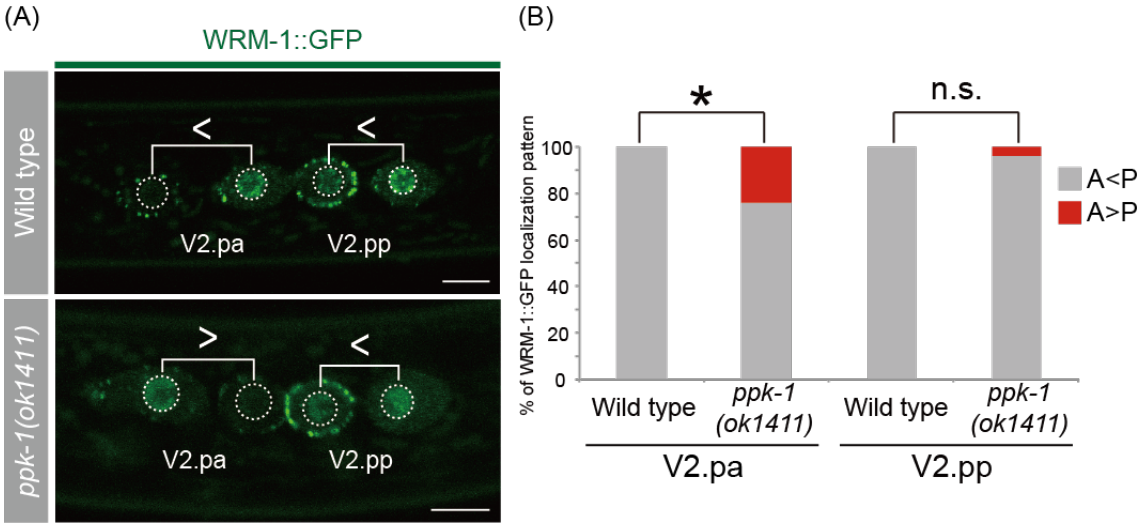

Figure 7. WRM-1 localization patterns in daughter nuclei in wild type and *ppk-1(ok1411)* mutants

(A) Confocal images showing the localization of WRM-1::GFP in wild type (top), and *ppk-1(ok1411)* (bottom). Pairs of daughter nuclei are shown with brackets for each panel. The inequality signs indicate relative intensities of WRM-1::GFP level between two daughters. Scale bars are 5 μm.

(B) Frequencies of the localization patterns of WRM-1::GFP in wild type (n=26) and *ppk-1* (n=25). A, intensity of WRM-1::GFP at the anterior nucleus; P, intensity of WRM-1::GFP at the posterior nucleus. *, $P<0.05$. n.s., not significant. Scale bar is 5 μm.

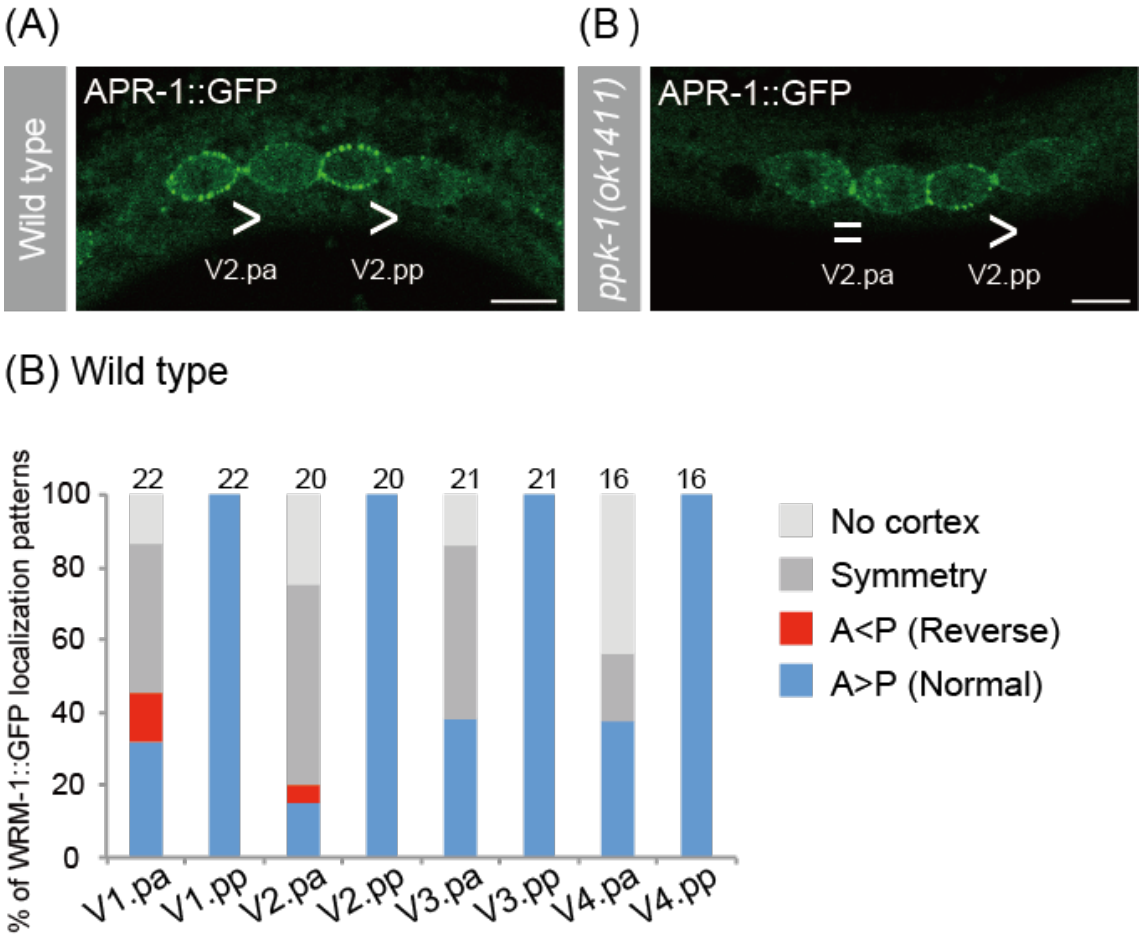

Figure 8. Cortical localization patterns of APR-1 and WRM-1

(A, B) Confocal images showing the localization of APR-1::GFP in the V2.pa and V2.pp cells of wild type(A, n=22) and *ppk-1(ok1411)*(B, n=11). The inequality signs indicate relative intensities of APR-1::GFP level between two daughters just after the division. Scale bars are 5 μm.

(B) Frequencies of the localization patterns of cortical WRM-1::GFP. The number of samples is shown above each column. The inequality signs indicate relative intensities of cortical WRM-1::GFP level between two daughters. No cortex means that WRM-1::GFP signal is absent from the cortex of the cells. Symmetry means that WRM-1::GFP localizes uniformly to the cortex.

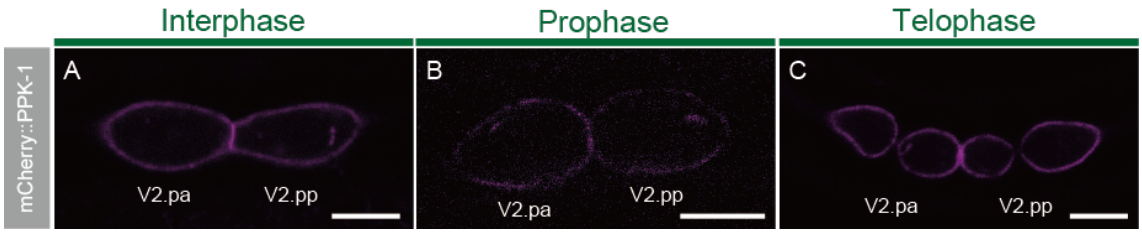

Figure 9. Intracellular localization patterns of PPK-1

(A-C) Confocal images showing the localization of mCherry::PPK-1 in the V2.pa and V2.pp cells of wild type at (A) interphase, (B) prophase, and (C) telophase. Scale bars are 5 μm.

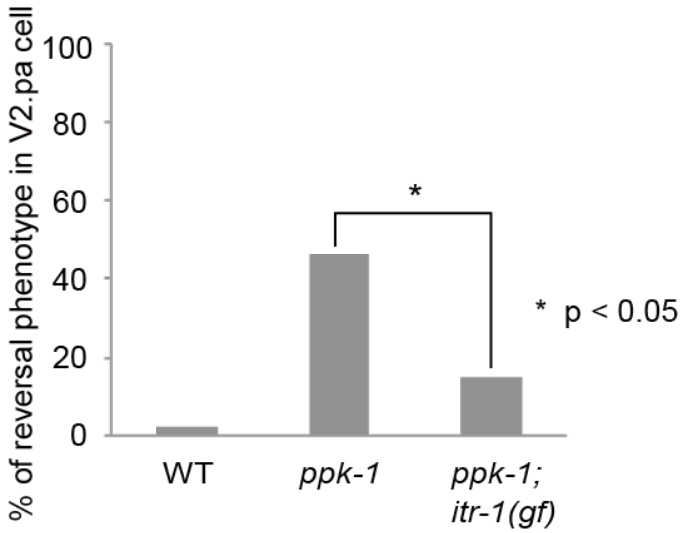

Figure 10. The *itr-1(gf)* mutation rescues reversal phenotype of V2.pa cell in *ppk-1* mutants

Frequencies of the reversal phenotype in V2.pa cell of wild type (n=81), *ppk-1(ok1411)* (n=50), and *ppk-1(ok1411)*; *itr-1(sy290,gf)* (n=20). *, P<0.05.

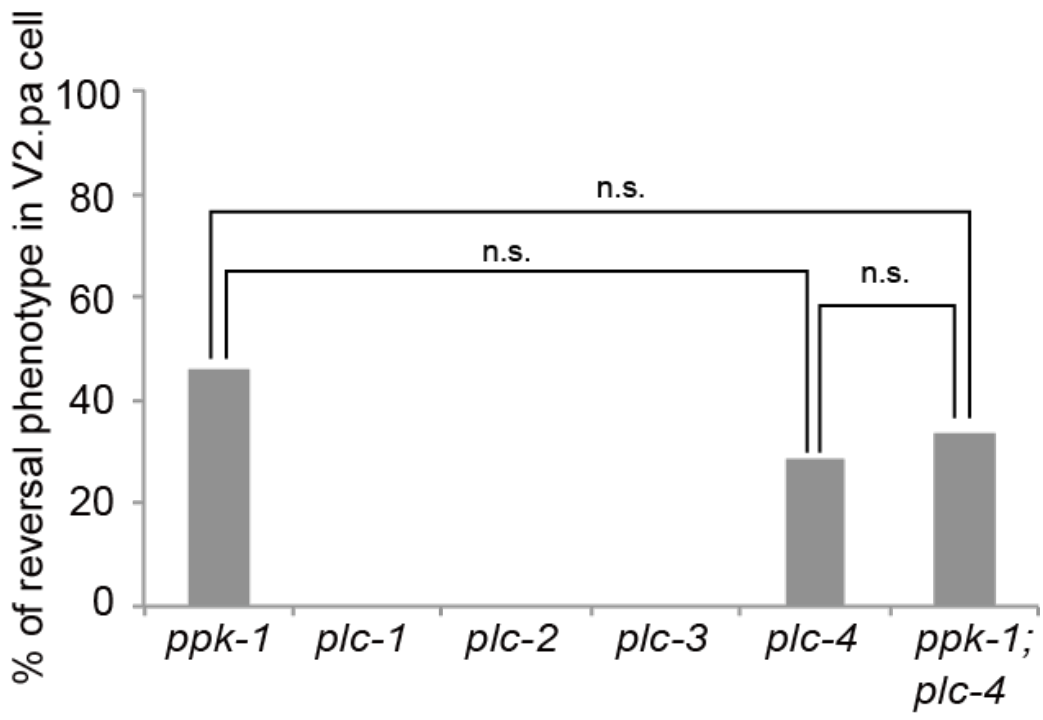

Figure 11. PLC-4 affects the ACD of the V2.pa cell.

Frequencies of the reversal phenotype in V2.pa cell of *ppk-1(ok1411)* (n=50), *plc-1(rx1)* (n=20), *plc-2(ok1761)* (n=21), *plc-3(tm1340)* (n=20), *plc-4(ok1215)* (n=35), *and ppk-1(ok1411); plc-4(ok1215)* (n=30). n.s., not significant.

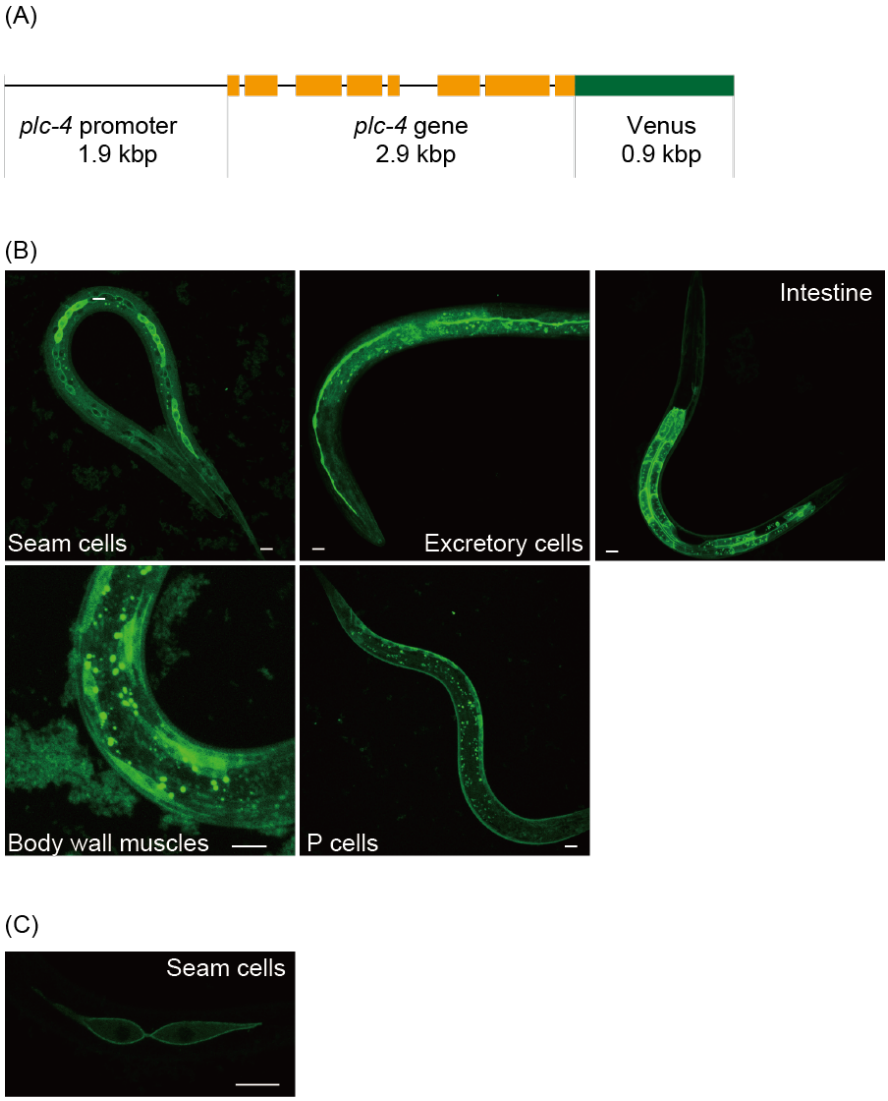

Figure 12. *plc-4::*Venus reporter experiment

(A) A schematic drawing of *Pplc-4::plc-4::*Venus.

(B) *plc-4* is expressed at high levels in seam cells, excretory cells, intestine, body wall muscles, and P cells. Scale bars are 5 μm.

(C) A magnified image of the seam cells that shows localization of PLC::Venus to the cell cortex.

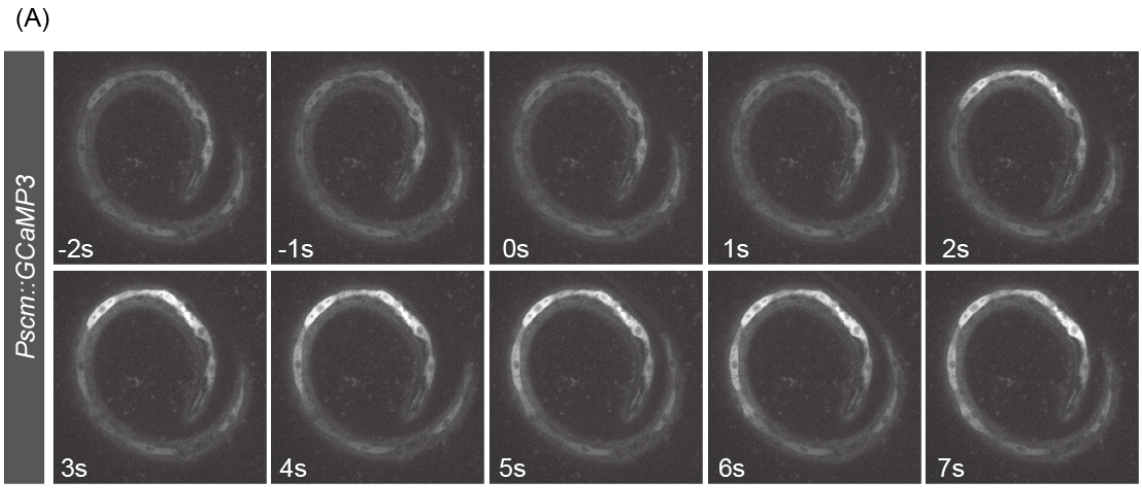

Figure 13. Calcium dynamics in seam cells

(A) Ten individual frames from time-lapse imaging of GCaMP3 wave in seam cells. 0s means start of Ca^{2+} wave.

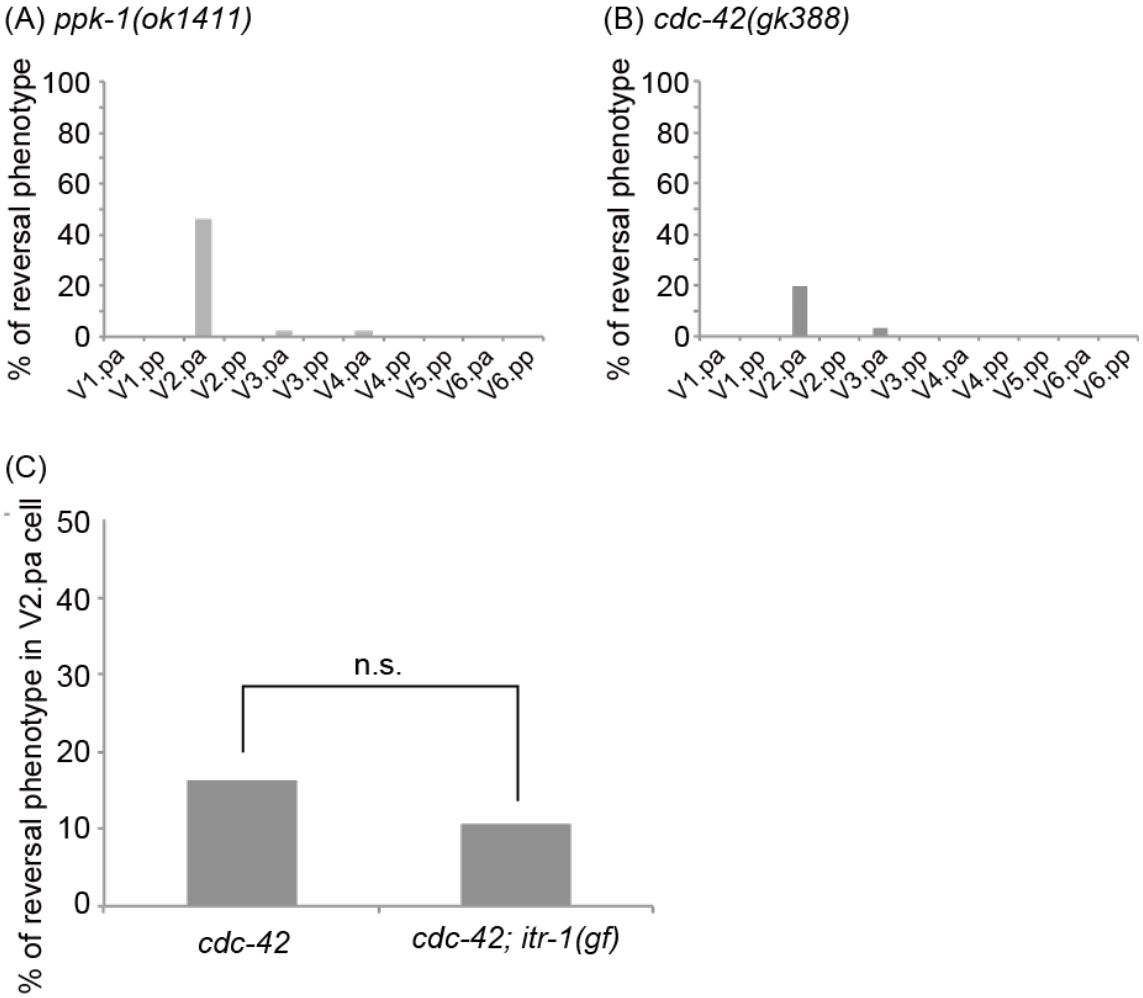

Figure 14. *cdc-42* may be a downstream effector of *itr-1*

(A) Frequencies of the reversal phenotype in *ppk-1(ok1411)* mutants at L2 stage (n=50).

(B) Frequencies of the reversal phenotype in *cdc-42(gk388)* mutants at L2 stage. (n=31)

(C) Frequencies of the reversal phenotype in V2.pa cell of *cdc-42(gk388)* (n=31) and *cdc-42(gk388); itr-1(sy290gf)* (n=56) . n.s., not significant

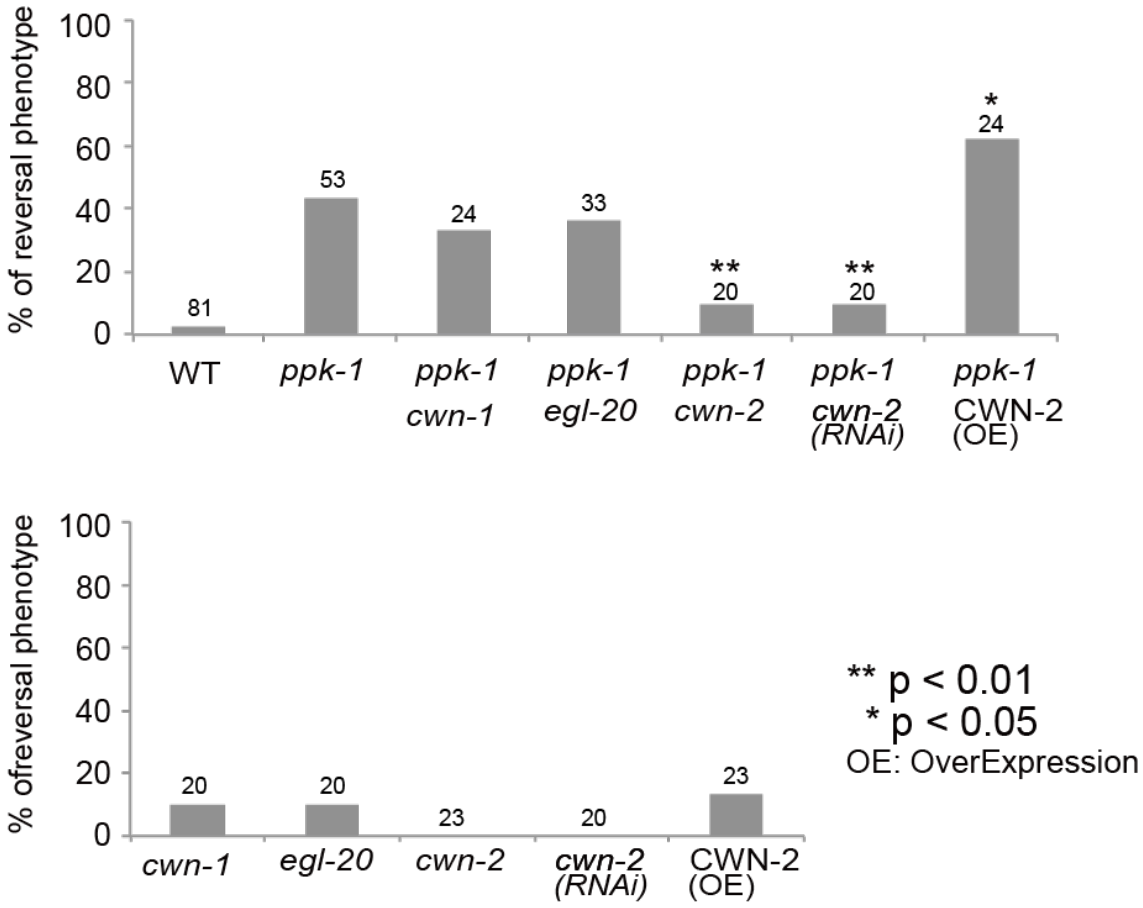

Figure 15. Genetic interaction analyses between *ppk-1* and Wnt genes

(A) A frequencies of the reversal phenotype in wild type, *ppk-1, ppk-1; cwn-1, ppk-1; egl-20, ppk-1; cwn-2, ppk-1; cwn-2(RNAi), ppk-1;Pcwn-2::*CWN-2::Venus, *cwn-1, egl-20, cwn-2, cwn-2(RNAi), and Pcwn-2::*CWN-2::Venus. Numbers of samples are shown above each column.

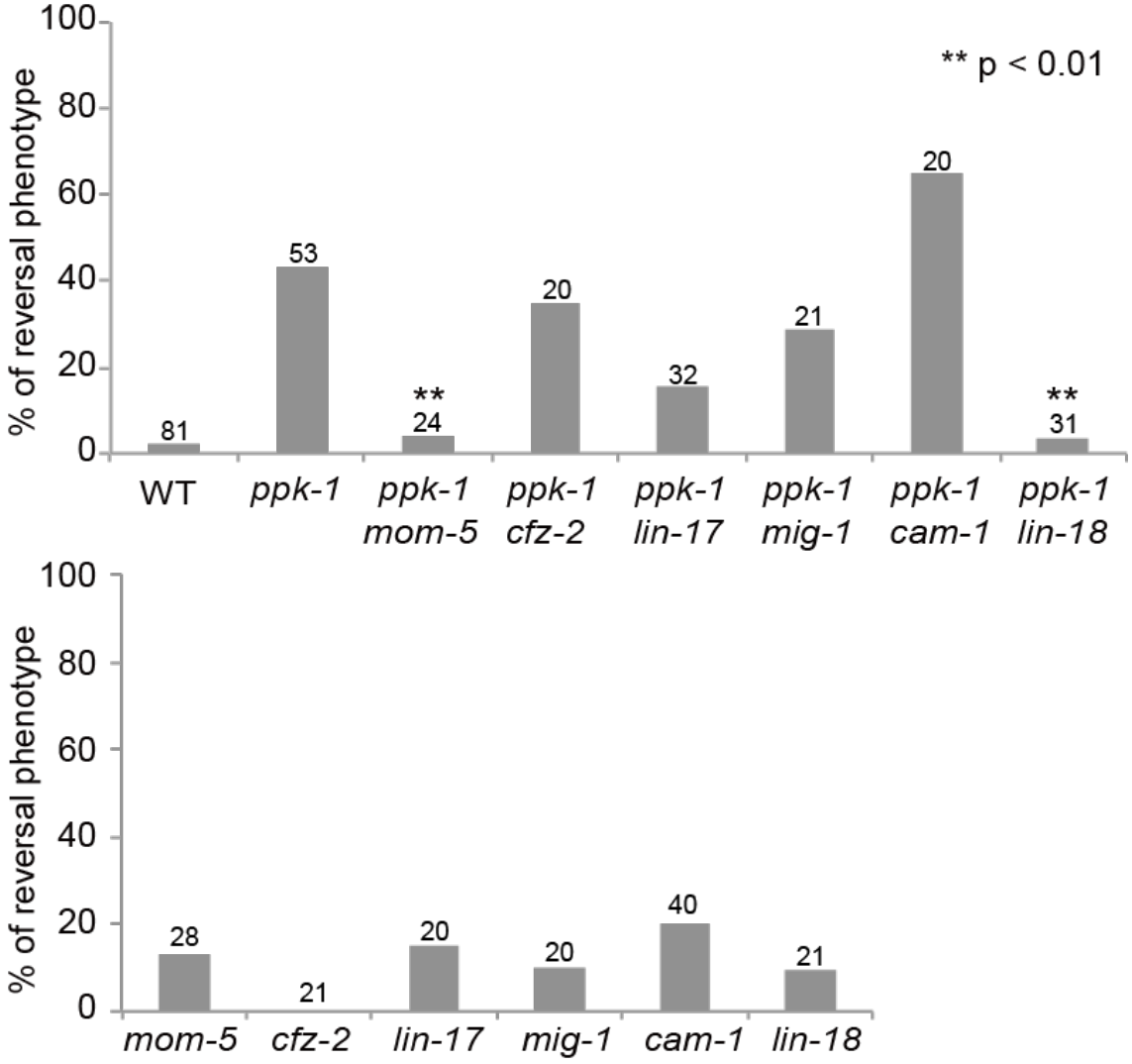

Figure 16. *ppk-1* phenotype partially depends on the amount of LIN-18.

Top: frequency of the reversal phenotype in *ppk-1(ok1411)* animals carrying *mom-5(ne12), cfz-2(ok1201), lin-17(n3091), mig-1(e1787), cam-1(ks52), and lin-18(e620)* mutations. Bottom: frequency of the reversal phenotype in *mom-5(ne12), cfz-2(ok1201), lin-17(n3091), mig-1(e1787), cam-1(ks52),* and *lin-18(e620).* **, P<0.01. Numbers of samples are shown above each column.

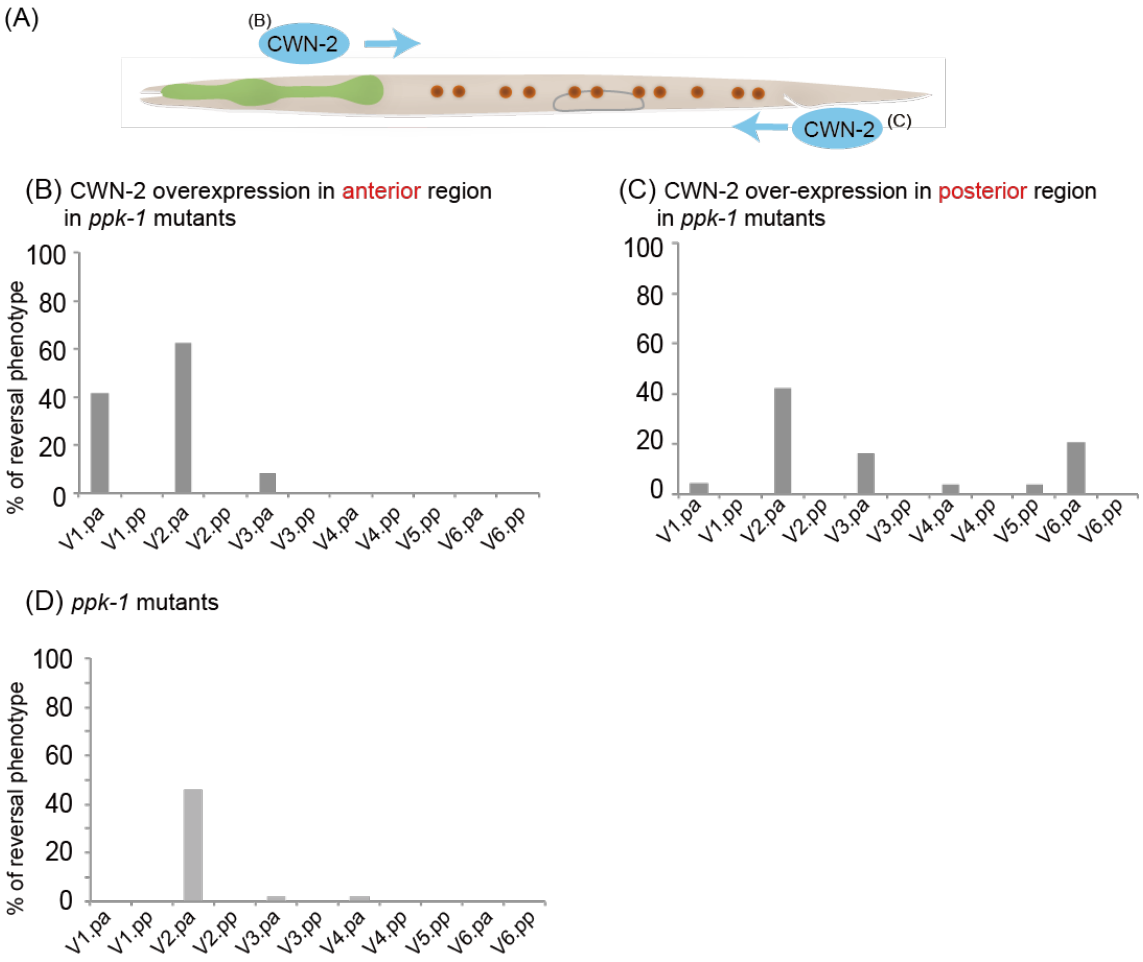

Figure 17. Overexpressed CWN-2 promotes the reversed polarity in *ppk-1* mutants

(A) A schematic drawing of positions in which CWN-2 is overexpressed

(B) Frequencies of the reversal phenotype in *ppk-1(ok1411)* animals carrying *Pcwn-2::*CWN-2*::*Venus (n=24)

(C) Frequencies of the reversal phenotype in *ppk-1(ok1411)* animals carrying *Pegl-20::*CWN-2*::*Venus (n=22)

(D) Frequencies of the reversal phenotype in *ppk-1* mutants (n=50)

(A) *cwn-1; egl-20 cwn-2*

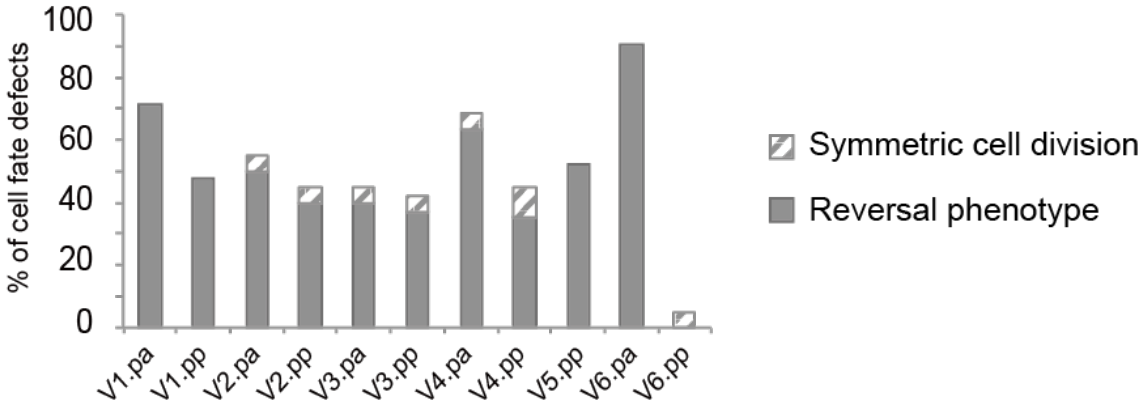

(B) *cwn-1; egl-20 cwn-2; Pegl-20::*CWN-2::Venus

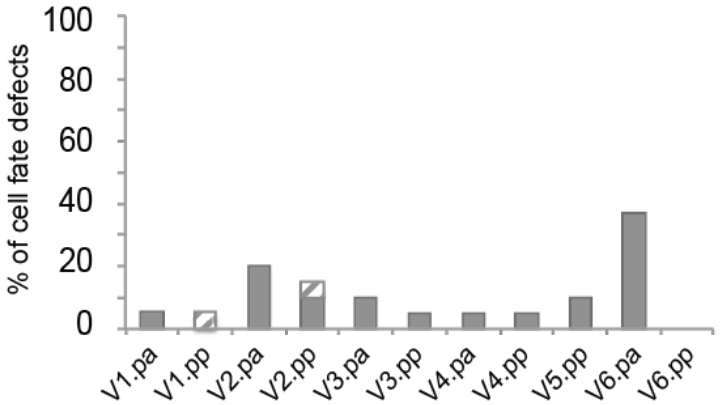

Figure 18. *Pegl-20::*CWN-2::Venus rescued the cell fate defects of triple Wnt mutants

(A) Frequencies of cell fate defects in triple Wnt mutants (*cwn-1(ok546); egl-20(n585) cwn-2(ok895)*). (n=21)

(B) Frequencies of cell fate defects in the triple Wnt mutants carrying *Pegl-20::CWN-2::*Venus. (n=23)

Figure 19

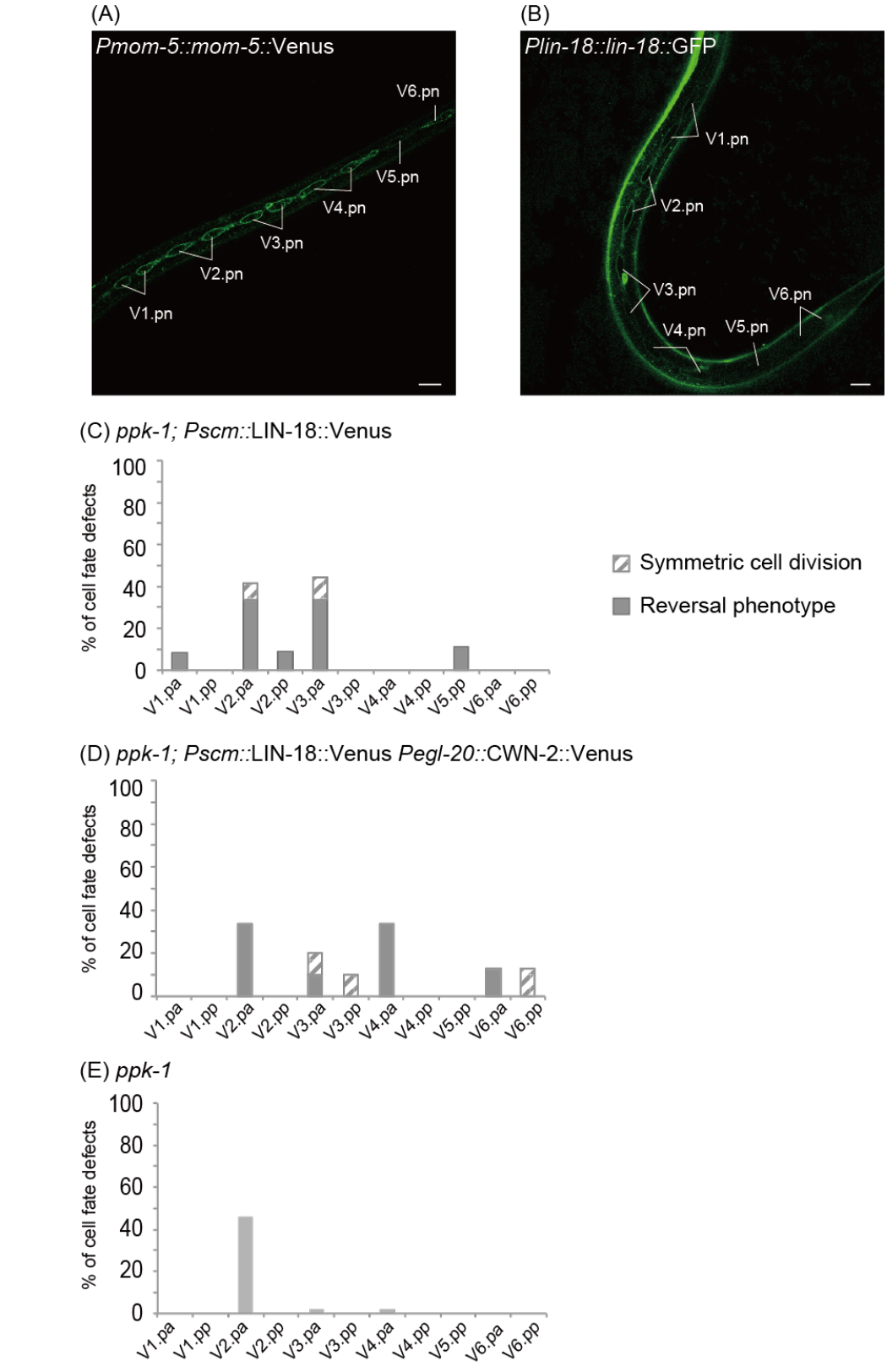
(A)
Pmom-5::mom-5::Venus
V6.pn
V5.pn
V4.pn
V3.pn
V2.pn
V1.pn
(B)
Plin-18::lin-18::GFP
V1.pn
V2.pn
V3.pn
V6.pn
V4.pn
V5.pn
(C) ppk-1; Pscm::LIN-18::Venus
% of cell fate defects
100
80
60
40
20
0
V1.pa
V1.pp
V2.pa
V2.pp
V3.pa
V3.pp
V4.pa
V4.pp
V5.pp
V6.pa
V6.pp
Symmetric cell division
Reversal phenotype
(D) ppk-1; Pscm::LIN-18::Venus Pegl-20::CWN-2::Venus
% of cell fate defects
100
80
60
40
20
0
V1.pa
V1.pp
V2.pa
V2.pp
V3.pa
V3.pp
V4.pa
V4.pp
V5.pp
V6.pa
V6.pp
(E) ppk-1
% of cell fate defects
100
80
60
40
20
0
V1.pa
V1.pp
V2.pa
V2.pp
V3.pa
V3.pp
V4.pa
V4.pp
V5.pp
V6.pa
V6.pp

Figure 19. Overexpressed LIN-18 promotes the reversed polarity in *ppk-1* mutants

(A) Confocal images showing the expression pattern of *Pmom-5::mom-5::*Venus(*osEx 524*). MOM-5 is expressed in all seam cells.

(B) Confocal images showing the expression pattern of *Plin-18::lin-18::*GFP(*syIs75*) (Inoue et al., 2004). LIN-18::GFP is expressed in seam cells that are located in the anterior side of the animals (from V1.pa to V3.pp cells) at the L2 stage.

(C) Frequencies of the cell fate defects in *ppk-1(ok1411)* animals carrying *Pscm::*LIN-18*::*Venus (n=24).

(D) Frequencis of the reversal phenotype in *ppk-1(ok1411)* animals carrying *cwn-2(ok895)* and *Pegl-20::CWN-2::*Venus (n=22).

(E) Frequencies of the reversal phenotype in *ppk-1* mutants (n=50).

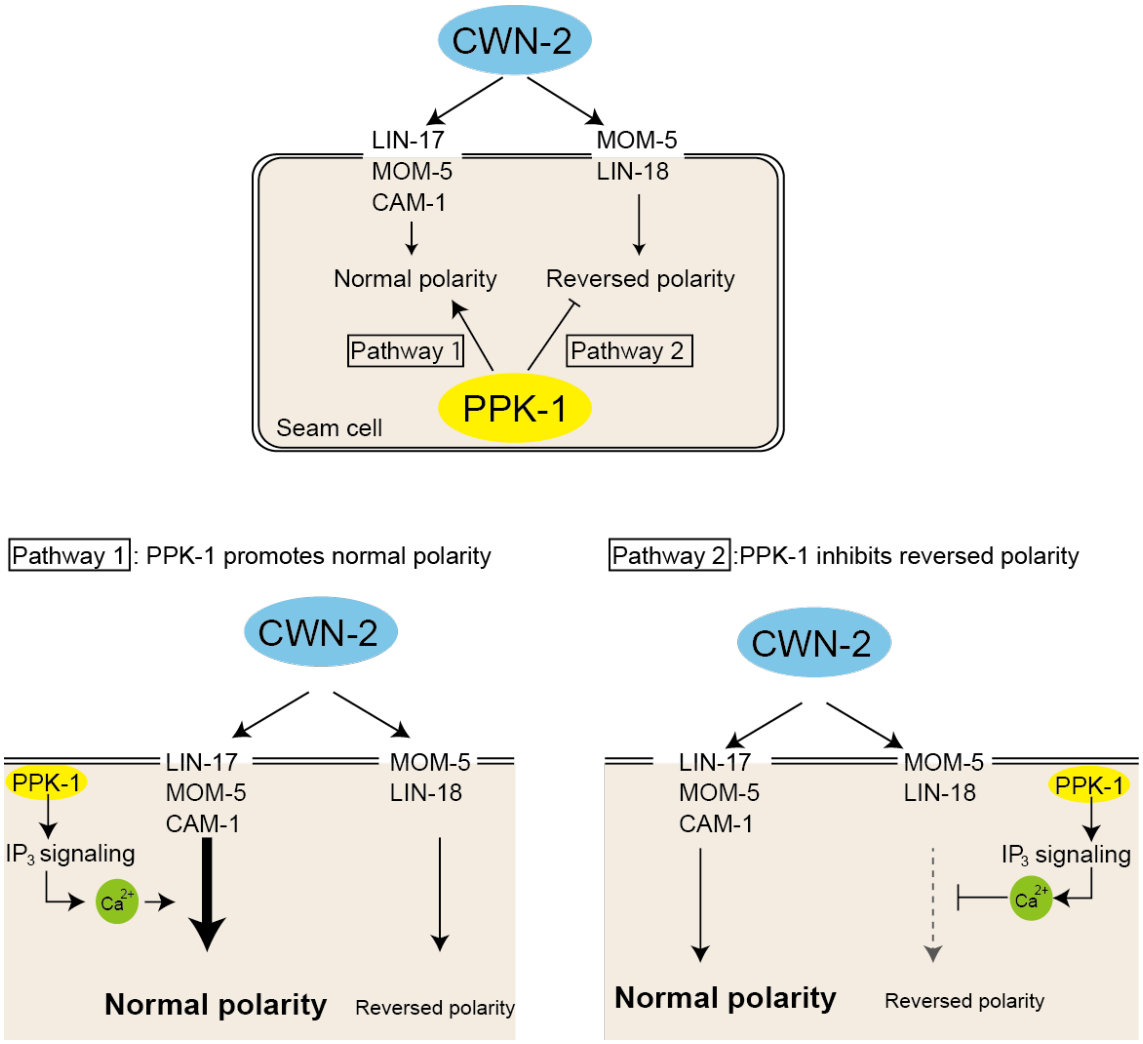

Figure 20. A model for the role of PPK-1 in the ACD

(A) CWN-2 promotes both normal and reversed polarities. PPK-1 is thought to have two functions. Pathway 1 is that PPK-1 promotes the normal polarity. Pathway 2 is that PPK-1 inhibits the reversed polarity.

(B and C) The details of Pathway 1 and Pathway 2.

References

Amon, A. (1996). Mother and daughter are doing fine: asymmetric cell division in yeast. Cell *84*, 651-654.

Bloom, L., and Horvitz, H.R. (1997). The *Caenorhabditis elegans* gene unc-76 and its human homologs define a new gene family involved in axonal outgrowth and fasciculation. Proceedings of the National Academy of Sciences of the United States of America *94*, 3414-3419.

Brenner, S. (1974). The genetics of *Caenorhabditis elegans*. Genetics *77*, 71-94.

Clandinin, T.R., DeModena, J.A., and Sternberg, P.W. (1998). Inositol trisphosphate mediates a RAS-independent response to LET-23 receptor tyrosine kinase activation in *C. elegans*. Cell *92*, 523-533.

Clapham, D.E. (2007). Calcium signaling. Cell *131*, 1047-1058.

Clevers, H. (2006). Wnt/beta-catenin signaling in development and disease. Cell *127*, 469-480.

Corrigan, C., Subramanian, R., and Miller, M.A. (2005). Eph and NMDA receptors control Ca2+/calmodulin-dependent protein kinase II activation during *C. elegans* oocyte meiotic maturation. Development *132*, 5225-5237.

Dal Santo, P., Logan, M.A., Chisholm, A.D., and Jorgensen, E.M. (1999). The inositol trisphosphate receptor regulates a 50-second behavioral rhythm in *C. elegans*. Cell *98*, 757-767.

Deshpande, R., Inoue, T., Priess, J.R., and Hill, R.J. (2005). lin-17/Frizzled and lin-18 regulate POP-1/TCF-1 localization and cell type specification during *C. elegans* vulval development. Developmental Biology *278*, 118-129.

Etienne-Manneville, S. (2004). Cdc42--the centre of polarity. Journal of Cell Science

117, 1291-1300.

Evans, J.H., and Falke, J.J. (2007). Ca^{2+} influx is an essential component of the positive-feedback loop that maintains leading-edge structure and activity in macrophages. Proceedings of the National Academy of Sciences of the United States of America *104*, 16176-16181.

Gilleard, J.S., Shafi, Y., Barry, J.D., and McGhee, J.D. (1999). ELT-3: A *Caenorhabditis elegans* GATA factor expressed in the embryonic epidermis during morphogenesis. Developmental Biology *208*, 265-280.

Goley, E.D., Toro, E., McAdams, H.H., and Shapiro, L. (2009). Dynamic chromosome organization and protein localization coordinate the regulatory circuitry that drives the bacterial cell cycle. Cold Spring Harbor Symposia on Quantitative Biology *74*, 55-64.

Gower, N.J., Walker, D.S., and Baylis, H.A. (2005). Inositol 1,4,5-trisphosphate signaling regulates mating behavior in *Caenorhabditis elegans* males. Molecular Biology of the Cell *16*, 3978-3986.

Horvitz, H.R., and Herskowitz, I. (1992). Mechanisms of asymmetric cell division: two Bs or not two Bs, that is the question. Cell *68*, 237-255.

Inoue, T., Oz, H.S., Wiland, D., Gharib, S., Deshpande, R., Hill, R.J., Katz, W.S., and Sternberg, P.W. (2004). *C. elegans* LIN-18 is a Ryk ortholog and functions in parallel to LIN-17/Frizzled in Wnt signaling. Cell *118*, 795-806.

Koh, K., and Rothman, J.H. (2001). ELT-5 and ELT-6 are required continuously to regulate epidermal seam cell differentiation and cell fusion in *C. elegans*. Development *128*, 2867-2880.

Laub, M.T., Shapiro, L., and McAdams, H.H. (2007). Systems biology of Caulobacter. Annual review of Genetics *41*, 429-441.

Lo, M.C., Gay, F., Odom, R., Shi, Y., and Lin, R. (2004). Phosphorylation by the beta-catenin/MAPK complex promotes 14-3-3-mediated nuclear export of TCF/POP-1 in signal-responsive cells in *C. elegans*. Cell *117*, 95-106.

Mello, C.C., Kramer, J.M., Stinchcomb, D., and Ambros, V. (1991). Efficient gene transfer in *C.elegans*: extrachromosomal maintenance and integration of transforming sequences. EMBO J *10*, 3959-3970.

Mizumoto, K., and Sawa, H. (2007). Cortical beta-catenin and APC regulate asymmetric nuclear beta-catenin localization during asymmetric cell division in *C. elegans*. Developmental Cell *12*, 287-299.

Nakamura, K., Kim, S., Ishidate, T., Bei, Y., Pang, K., Shirayama, M., Trzepacz, C., Brownell, D.R., and Mello, C.C. (2005). Wnt signaling drives WRM-1/beta-catenin asymmetries in early *C. elegans* embryos. Genes & Development *19*, 1749-1754.

Pilipiuk, J., Lefebvre, C., Wiesenfahrt, T., Legouis, R., and Bossinger, O. (2009). Increased IP3/Ca^{2+} signaling compensates depletion of LET-413/DLG-1 in *C. elegans* epithelial junction assembly. Developmental Biology *327*, 34-47.

Schlessinger, K., McManus, E.J., and Hall, A. (2007). Cdc42 and noncanonical Wnt signal transduction pathways cooperate to promote cell polarity. The Journal of Cell Biology *178*, 355-361.

Sheldahl, L.C., Slusarski, D.C., Pandur, P., Miller, J.R., Kuhl, M., and Moon, R.T. (2003). Dishevelled activates Ca2+ flux, PKC, and CamKII in vertebrate embryos. The Journal of Cell Biology *161*, 769-777.

Siegfried, K.R., Kidd, A.R., 3rd, Chesney, M.A., and Kimble, J. (2004). The sys-1 and sys-3 genes cooperate with Wnt signaling to establish the proximal-distal axis of the *Caenorhabditis elegans* gonad. Genetics *166*, 171-186.

Sulston, J.E., and Horvitz, H.R. (1977). Post-embryonic cell lineages of the nematode,

Caenorhabditis elegans. Developmental Biology *56*, 110-156.

Takeshita, H., and Sawa, H. (2005). Asymmetric cortical and nuclear localizations of WRM-1/beta-catenin during asymmetric cell division in *C. elegans*. Genes & Development *19*, 1743-1748.

Thomas-Virnig, C.L., Sims, P.A., Simske, J.S., and Hardin, J. (2004). The inositol 1,4,5-trisphosphate receptor regulates epidermal cell migration in *Caenorhabditis elegans*. Current Biology : CB *14*, 1882-1887.

Tian, L., Hires, S.A., Mao, T., Huber, D., Chiappe, M.E., Chalasani, S.H., Petreanu, L., Akerboom, J., McKinney, S.A., Schreiter, E.R.*, et al.* (2009). Imaging neural activity in worms, flies and mice with improved GCaMP calcium indicators. Nature Methods *6*, 875-881.

Vazquez-Manrique, R.P., Legg, J.C., Olofsson, B., Ly, S., and Baylis, H.A. (2010). Improved gene targeting in *C. elegans* using counter-selection and Flp-mediated marker excision. Genomics *95*, 37-46.

Walker, D.S., Ly, S., Gower, N.J., and Baylis, H.A. (2004). IRI-1, a LIN-15B homologue, interacts with inositol-1,4,5-triphosphate receptors and regulates gonadogenesis, defecation, and pharyngeal pumping in *Caenorhabditis elegans*. Molecular Biology of the Cell *15*, 3073-3082.

Walker, D.S., Vazquez-Manrique, R.P., Gower, N.J., Gregory, E., Schafer, W.R., and Baylis, H.A. (2009). Inositol 1,4,5-trisphosphate signalling regulates the avoidance response to nose touch in *Caenorhabditis elegans*. PLoS Genetics *5*, e1000636.

Wallingford, J.B., Ewald, A.J., Harland, R.M., and Fraser, S.E. (2001). Calcium signaling during convergent extension in *Xenopus*. Current Biology : CB *11*, 652-661.

Walston, T., Tuskey, C., Edgar, L., Hawkins, N., Ellis, G., Bowerman, B., Wood, W., and Hardin, J. (2004). Multiple Wnt signaling pathways converge to orient the mitotic

spindle in early *C. elegans* embryos. Developmental Cell *7*, 831-841.

Wei, C., Wang, X., Chen, M., Ouyang, K., Song, L.S., and Cheng, H. (2009). Calcium flickers steer cell migration. Nature *457*, 901-905.

Weinkove, D., Bastiani, M., Chessa, T.A., Joshi, D., Hauth, L., Cooke, F.T., Divecha, N., and Schuske, K. (2008). Overexpression of PPK-1, the *Caenorhabditis elegans* Type I PIP kinase, inhibits growth cone collapse in the developing nervous system and causes axonal degeneration in adults. Developmental Biology *313*, 384-397.

Xu, S., and Chisholm, A.D. (2011). A Galphaq-Ca^{2+} signaling pathway promotes actin-mediated epidermal wound closure in *C. elegans*. Current Biology : CB *21*, 1960-1967.

Xu, X., Guo, H., Wycuff, D.L., and Lee, M. (2007). Role of phosphatidylinositol-4-phosphate 5' kinase (*ppk-1*) in ovulation of *Caenorhabditis elegans*. Exp Cell Res *313*, 2465-2475.

Yamamoto, Y., Takeshita, H., and Sawa, H. (2011). Multiple Wnts redundantly control polarity orientation in *Caenorhabditis elegans* epithelial stem cells. PLoS Genetics *7*, e1002308.

My publications

NMR analyses of the interaction between the FYVE domain of early endosome antigen 1 (EEA1) and Phosphoinositides embedded in a lipid bilayer.

Yokogawa M, Kobashigawa Y, Yoshida N, Ogura K, Harada K, Inagaki F.

J Biol Chem. 2012 Oct 12;287(42):34936-45.

Phosphoinositide-incorporated lipid-protein nanodiscs: A tool for studying protein-lipid interactions.

Kobashigawa Y, Harada K, Yoshida N, Ogura K, Inagaki F.

Anal Biochem. 2011 Mar 1;410(1):77-83.

Solution structure of a novel Cdc42 binding module of Bem1 and its interaction with Ste20 and Cdc42.

Takaku T, Ogura K, Kumeta H, Yoshida N, Inagaki F.

J Biol Chem. 2010 Jun 18;285(25):19346-53.

Acknowledgements

The work described in this thesis has been carried out under the direction of Professor Hitoshi Sawa. I would like to extend my deep gratitude to Professor Hitoshi Sawa for his mentorship, suggestion, and encouragement for whole work.

I am truly thankful to Professor Takehiko Kobayashi and Associate Professor Daiju Kitagawa for their understanding and support for the completion my study. I would like to express my appreciation to Professor Hiroyuki Arai, Professor Yasushi Hiromi, Associate Professor Shinya Miyagishima, and Professor Yumiko Saga for valuable suggestions about my work. I wish to thank Associate Professor Shinji Ihara for valuable suggestions and for teaching me many experimental techniques about *C. elegans*. I also thank to Dr. Sohei Nakayama for enthusiastic discussions and for teaching me the many types of fluorescent proteins.

This thesis could not have been realized without the considerable help from the following people: Dr. Shuhei So, Mr. Kyohei Uemura, Mr. Kiyotaka Matsuzawa, Dr. Yinhua Jin, Ms. Masako Yokoo, Ms. Kayo Nakajima, and Ms. Yuriko Konagaya. The author is grateful to all the past and present members of the Department of Multicellular Organization Lab. , National Institute of Genetics.

Finally, I express special thanks to my parents and friends who have always supported me.

March 2015